การวิเคราะห์การกลายพันธุ์ และการศึกษาผลของการกลายพันธุ์ต่อการทำหน้าที่ของยีน *DcR3* ในผู้ป่วยโรค SLE

นายชญานิน โชคดีมีบุญ

วิทยานิพนธ์นี้เป็นส่วนหนึ่งของการศึกษาตามหลักสูตรปริญญาวิทยาศาสตรดุษฎีบัณฑิต
สาขาวิชาชีวเวชศาสตร์ (สหสาขาวิชา)
บัณฑิตวิทยาลัย จุฬาลงกรณ์มหาวิทยาลัย
ปีการศึกษา 2554

MUTATION ANALYSES AND FUNCTIONAL STUDIES OF *DcR3* IN PATIENTS WITH SLE

Mr. Chayanin Chokdeemeeboon

A Dissertation Submitted in Partial Fulfillment of the Requirements

for the Degree of Doctor of Philosophy Program in Biomedical Sciences

(Interdisciplinary Program)

Graduate School

Chulalongkorn University

Academic Year 2011

Thesis Title	MUTATION ANALYSES AND FUNCTIONAL SYUDIES OF *DcR3* IN PATIENTS WITH SLE
By	Mr. Chayanin Chokdeemeeboon
Field of Study	Biomedical Sciences
Thesis Advisor	Professor Vorasuk Shotelersuk, MD.
Thesis Co-advisor	Associate Professor Kanya Suphapeetiporn, MD., Ph.D.

Accepted by the Graduate School, Chulalongkorn University in Partial Fulfillment of the Requirements for the Doctoral Degree

…….. Dean of the Graduate School
(Associate Professor Pornpote Piumsomboon, Ph.D.)

THESIS COMMITTEE

…….. Chairman
(Professor Apiwat Mutirangura, MD., Ph.D.)

…….. Thesis Advisor
(Professor Vorasuk Shotelersuk, MD)

…….. Thesis Co-advisor
(Associate Professor Kanya Suphapeetiporn, MD., Ph.D.)

…….. Examiner
(Associate Professor Nattiya Hirankarn, MD., Ph.D.)

…….. Examiner
(Associate Professor Voravee Hoven, Ph.D.)

…….. External Examiner
(Ponpan Matangkasombut Choopong, MD., SD.)

ชญานิน โชคดีมีบุญ : การวิเคราะห์การกลายพันธุ์ และการศึกษาผลของการกลายพันธุ์ต่อการทำหน้าที่ของยีน *DcR3* ในผู้ป่วยโรค SLE (MUTATION AND FUNCTIONAL STUDIES OF *DcR3* IN PATIENTS WITH SLE) อ. ที่ปรึกษาวิทยานิพนธ์หลัก : ศ. นพ. วรศักดิ์ โชติเลอศักดิ์, อ. ที่ปรึกษาวิทยานิพนธ์ร่วม : รศ. พญ. ดร. กัญญา ศุภปีติพร, 78 หน้า.

SLE เป็นโรคพหุปัจจัย ถึงแม้ว่ามียีนหลายยีนที่เกี่ยวข้องกับการเกิดโรค แต่ยังมีอีกหลายยีนที่ยังไม่ถูกค้นพบ จากการศึกษาซึ่งพบว่าหนูที่มีการแสดงออกของยีน *DcR3* ของมนุษย์ มีลักษณะคล้ายกับโรค SLE ในมนุษย์ และในผู้ป่วยโรค SLE พบระดับของโปรตีน DcR3 เพิ่มขึ้นในซีรั่ม นำไปสู่สมมติฐานว่าผู้ป่วยโรค SLE จำนวนหนึ่งอาจจะมีการกลายพันธุ์ของยีน *DcR3* แบบ gain-of-function คณะผู้วิจัยจึงได้ทำการถอดรหัสพันธุกรรมของยีน *DcR3* ในผู้ป่วยโรค SLE จำนวน 200 คน และพบการกลายพันธุ์แบบ heterozygous missense (p.T56I และ p.H122Y) ในผู้ป่วย 2 คนซึ่งได้รับการถ่ายทอดมาจากแม่ที่ไม่เป็นโรค SLE มีหลักฐานหลายประการบ่งชี้ว่าการกลายพันธุ์มีบทบาทต่อการเกิดโรค จากประชากรกลุ่มควบคุม 500 คน พบการกลายพันธุ์แบบ p.H122Y จำนวน 1 คน ในขณะที่ไม่พบการกลายพันธุ์แบบ p.T56I เลย การกลายพันธุ์ทั้งสองเปลี่ยนขั้วของกรดอะมิโน และอยู่ในตำแหน่งที่โปรตีนจับกับโมเลกุลของ Fas ligand กรดอะมิโนตำแหน่งที่ 56 มีการอนุรักษ์ในสัตว์ที่มีกระดูกสันหลัง 14 สายพันธุ์ จากการศึกษาโดยใช้ surface plasmon resonance พบว่าการกลายพันธุ์แบบ p.T56I มีการจับกับ FasL เพิ่มขึ้น 2.4 เท่า ในขณะที่ p.H122Y ลดลง 0.7 เท่า ด้วยวิธี AnnexinV/PI staining ไม่พบความแตกต่างของความสามารถในการยับยั้ง FasL-induced apoptosis ใน Jurkat cells และ activation induced cell death ใน lymphocytes ระหว่าง DcR3 แบบปกติ และ DcR3 แบบกลายพันธุ์ เป็นที่น่าสนใจเมื่อใช้วิธี [^{3}H] thymidine incorporation พบว่า DcR3 ที่กลายพันธุ์ทั้งสองแบบเพิ่ม lymphocyte proliferation ได้อย่างมีนัยสำคัญทางสถิติเมื่อเทียบกับ DcR3 แบบปกติ โดยสรุปคณะผู้วิจัยได้ค้นพบการกลายพันธุ์ของยีน *DcR3* 2 แบบซึ่งอาจมีบทบาทในการเกิดโรค SLE ในมนุษย์

สาขาวิชา ชีวเวชศาสตร์ ลายมือชื่อนิสิต.....

ปีการศึกษา 2554 ลายมือชื่อ อ.ที่ปรึกษาวิทยานิพนธ์หลัก.....

ลายมือชื่อ อ.ที่ปรึกษาวิทยานิพนธ์ร่วม.....

5087870420 : MAJOR BIOMEDICAL SCIENCES

KEYWORDS : SLE / DcR3 / Mutation / Apoptosis / FasL/ Proliferation

CHAYANIN CHOKDEEMEEBOON: MUTATION AND FUNCTIONAL STUDIES OF *DcR3* IN PATIENTS WITH SLE. ADVISOR: PROF. VORASUK SHOTELERSUK, M.D., CO-ADVISOR: ASSOC. PROF. KANYA SUPHAPEETIPORN, M.D., Ph.D., 78 pp.

SLE is a multifactorial disorder. Although several of its underlying genes have been identified, many more remain to be discovered. The fact that *DcR3* transgenic mice had phenotypes similar to human SLE and SLE patients had an increased level of serum DcR3 has led us to hypothesize that a proportion of SLE patients might have a *DcR3* gain-of-function mutation. Here, we performed PCR-sequencing of the entire coding regions of *DcR3* in 200 unrelated SLE patients and found two heterozygous missense mutations (p.T56I and p.H122Y) in two patients. They inherited these from their unaffected mothers. Many lines of evidence suggest their etiologic role. Of the 500 controls, the p.H122Y was present in one control, while the p.T56I was absent. Both mutations changed polarity of the amino acid residues and resided in the Fas ligand binding domain. The amino acid residue 56th was conserved in 14 vertebrate species. Using surface plasmon resonance assay, we found that the p.T56I mutant had a 2.4 fold greater, whereas the p.H122Y had 0.7 fold lower affinity to FasL. AnnexinV/PI staining assays showed no differences of the ability to suppress FasL-induced Jurkat apoptosis and activation-induced cell death in lymphocytes between the *DcR3* mutants and the wild-type. Interestingly, using [^{3}H] thymidine incorporation assay, we found that both *DcR3* mutants statistically significantly increased lymphocyte proliferation more than that of the wild-type. In summary, for the first time, we identified two *DcR3* mutations that might play an etiologic role in human SLE pathogenesis.

Field of Study : BIOMEDICAL SCIENCES Student's Signature .....

Academic Year : 2011 Advisor's Signature .....

Co-advisor's Signature .....

ACKNOWLEDGEMENTS

I am very grateful to my supervisors, Professor Vorasuk Shotelersuk and Associate Professor Kanya Suphapeetiporn who endowed scientific knowledge and skills for me to complete this dissertation. They also encouraged me in doing right thing and gave me moral support.

I am indebted to Professor Apiwat Mutirangura, a director of Biomedical Sciences program, who gave me an opportunity to study in Ph.D. program.

I would like to show my gratitude to Associate Professor Nattiya Hirankarn who generously provided me with a lot of academic research knowledge and Associate Professor Voravee P. Hoven who supported me in performing SPR experiment as an important part in this dissertation.

I am pleased to thank Professor Steven Edwards who gave me an opportunity to perform some parts of the dissertation in School of Biological Sciences, University of Liverpool.

It is a pleasure to thank Mr.Pramuk Ammarinthnukrowh who is a person initiating the idea for this dissertation and thank to Dr.Helen Wright, Dr.Connie Lam, Dr.Petcharat Leoyklang, Dr.Piyaporn Akkahat, Dr.Supranee Buranapraditkun, Ms.Wanwimon Mekboonsonglarp, Ms.Oraphan Wiarachai, Ms.Ratchada Intwattana, Ms.Siraprapa Tongkobpetch, and Mr.Chalurmpon Srichomtong who kindly gave me good advice and support to perform some experiments as crucial parts in this dissertation.

This is a great opportunity to express my respect to Dr. Ponpan Matangkasombut Choopong for being a committee of this dissertation.

This dissertation was supported by Chulalongkorn University Dutsadi Phiphat Scholarship and Chulalongkorn University Graduate Scholarship to commemorate the 72th Anniversary of His Majesty the King Bhumibol Adulyadej.

This dissertation is dedicated to my parents, members of my family and all of my beloved friends.

CONTENTS

Page

LIST OF TABLES

LIST OF FIGURES

LIST OF ABBREVIATIONS

AICD	Activation induced cell death
ALPS	Autoimmune lymphoproliferative syndrome
CRD	Cysteine-rich domain
DcR3	Decoy receptor 3
DNASE1L3	Deoxyribonuclease I-like 3
dNTP	Deoxyribonucleotide triphosphate
EDC	Ethyldimethylaminopropyl carbodiimide
FasL	Fas ligand
GFP	Green fluorescence protein
HBD	Heparan binding domain
HVEM	Herpesvirus entry mediator
ITGAL	Integrin alpha L
ITGAM	Integrin alpha M
LIGHT	homologous to lymphotoxins, exhibits inducible expression, and competes with HSV glycoprotein D for HVEM on T cells
NHS	*N*-Hydroxysuccinimide

PCR	Polymerase chain reaction
PHA	Phytohaemagglutinin
PolyPhen	Polymorphism phenotyping
PPP2CA	Protein phosphatase 2 catalytic subunit alpha isozyme
PTPN22	Protein tyrosine phosphatase non-receptor type 22
RA	Rheumatoid arthritis
RFLP	Restriction fragment length polymorphism
SLE	Systemic lupus erythematosus
SLEDAI	SLE disease activity index
SP	Signal peptide
SPR	Surface plasmon resonance
TL1A	TNF-like cytokine 1A
TLR7	Toll-like receptor 7
TNFRS6B	Tumor necrosis factor receptor superfamily member 6B
TREX1	Three prime repair exonuclease 1

CHAPTER I

INTRODUCTION

Background and significance

Systemic lupus erythematosus (SLE) is a complex autoimmune disease characterized by autoantibody production and tissue injury from the immune complexes with multi-organ involvement. SLE shows diverse clinical manifestations. Diagnosis of SLE requires at least 4 of 11 criteria established by American College of Rheumatology. SLE is a chronic disease that can be life threatening if the important organs are affected [1]. In juvenile SLE, there is an even gender ratio in children younger than 2 years old and the female to male ratio is 4:3 during the first decade of life [2]. In adult SLE, the female to male ratio is 9:1 and decreases to 5:1 at the age after 50 years [3-5]. There are several factors involving SLE pathogenesis consisting of genetic, epigenetic, environmental, and hormonal factors [6]. Smoking, exposure to ultraviolet, and Epstein-Barr virus infection are the environmental factors contributing to SLE [7-10]. Epigenetic changes in some genes are known to be associated with SLE pathogenesis [6]. In a murine model, mice supplemented with estrogen or prolactin develop autoimmune with an increase in the autoreactive B-cells [11]. In human, SLE is much more prevalent in women of childbearing age and the level of estradiol is higher; whereas testosterone is lower in men with SLE in comparison to healthy controls [12].

Several lines of evidence show that genetic factors contribute to SLE. The disease is exhibited by familial clustering with 10 to 12 percent of SLE patients in the first-degree relative and a high risk sibling ratio (λ_s=8-29) [13]. In addition, the concordance rate in monozygotic (>24-58%) is much higher than dizygotic twins (2-5%) in SLE [14]. So far, there are at least 56 genes distributing among 17 chromosomes including X chromosome identified to be associated with SLE [6].

A number of genes have been implicated in SLE. They can be classified into three categories on the basis of their physiological functions. The first category

composes of genes involving in mechanisms of dead and dying cells elimination. Defects in these genes provide a source of autoantigen triggering autoimmunity. The second category includes genes encoding proteins that regulate the activation and tolerance of T and B lymphocytes, such as *Fas*, and *FasL*. The third category is a group of genes that could modify the expression of SLE in individual organs by their involvement in immune complex-mediated inflammation. For example, polymorphisms in *FcγRIIa* and *FcγRIIIa* are thought to differ in their ability to bind to immune complexes and are associated with the presence of nephritis in SLE [15].

In 2007, there was a study showing that human-*DcR3* transgenic mice developed SLE-like syndrome. Intriguingly, SLE-like syndrome showed higher penetrance in female (~60%) than in male (20%) mice. In addition, some of wild type mice (5/8) that were transplanted with bone marrow of human-*DcR3* transgenic mice developed SLE-like syndrome [16]. .A year later, DcR3 has been reported as a new diagnostic parameter and risk factor for SLE [17]. There are three studies demonstrating that the level of serum DcR3 significantly increased in SLE patients in comparison to healthy controls [17-19]. One study showed that DcR3 reduced activation induced cell death (AICD) in T cells and enhanced T cell proliferation suggesting that DcR3 possibly plays a pathogenic role in SLE [19]. Although DcR3 is a soluble decoy receptor that blocks at least three apoptotic signaling pathways consisting of FasL/Fas, LIGHT/HVEM-LTBR, and TL1A/DR3, the blocking of FasL/Fas pathway is most likely relevant to SLE pathogenesis because mice with the *FasL* and *Fas* gene defects exhibited autoimmune disease [20, 21] and mutations in the *FasL* and *Fas* gene resulted in decreased activation induced cell death. In addition, increased T cell proliferation were identified in patients with SLE [22, 23]. There was no SLE phenotype observed in LIGHT-null and DR3-null mice [16, 24, 25]. Although, the amount of serum DcR3 increased in the SLE patients, not all SLE patients showed detectable serum DcR3. Therefore, the role of DcR3 in SLE pathogenesis might not be only the increased level of serum DcR3, but it might also be other defects particularly in the defect of protein function resulted from *DcR3* gene mutations.

In this study, we firstly measured the level of serum DcR3 in juvenile SLE patients. We found that the level of serum DcR3 was elevated in juvenile SLE patients in consistence with the previous studies [17, 19]. The proportion of juvenile SLE patients had the elevated level of serum DcR3, while some had normal levels of serum DcR3. Theoretically, genetic factors rather contribute to the multi-factorial diseases in the early onset patients and we were studying DcR3 defect in juvenile SLE. In addition to increased level of serum DcR3, there might be mutations in the *DcR3* gene which contribute to SLE pathogenesis in our juvenile SLE patients. Therefore, we did PCR-sequencing in entire coding regions of *DcR3* in one hundred juvenile SLE patients. We identified one heterozygous c.C364T mutation in a juvenile SLE patient. Then, we further identified whether the mutation could also be found in adult SLE. We did PCR-sequencing in the *DcR3* gene in one hundred adult SLE patients (genomic DNA obtained from Lupus Research Unit, Faculty of Medicine, Chulalongkorn University). We identified one other heterozygous c.C167T mutation in one adult SLE patient. Both of them were missense mutations resulting in amino acids substitution at positions 56 (threonine to isoleucine) and 122 (histidine to tyrosine). Both substitutions affect protein primary structure and the group of substituted amino acids also change. Intriguingly, both mutations resided in the FasL binding domains suggesting the mutant proteins might change affinity to FasL. The amino acid residue 56 is conserved in 14 vertebrate species, while the 122 is conserved among 5 mammalian species (results shown in figure 11A and B in Chapter IV). The impact of mutations on protein function was predicted to be probably and possibly damaging respectively by PolyPhen. The mutant alleles were investigated whether they were found in unaffected controls. There was no c.C167T allele; whereas, there was one c.C364T allele in 1,000 alleles from 500 ethnic-matched unaffected controls. Although one allele of c.C364T was found in unaffected controls, the allele frequency was very low (0.1%). So, we investigated whether the mutations in the *DcR3* gene affected its protein function. We then conducted affinity test of the wild type and mutant DcR3 to FasL. In addition, the biological functions of mutant

DcR3 consisting of Jurkat cell apoptosis, lymphocyte apoptosis and lymphocyte proliferation were conducted in this study.

Research questions

1. Are there mutations in the *DcR3* gene expected to affect its primary protein structures in SLE patients?

2. Do these DNA changes of the *DcR3* gene affect its protein functions?

Objectives

1. To identify mutations in the *DcR3* gene expected to affect its primary protein structures in SLE patients

2. To determine whether these DNA changes of the *DcR3* gene affect its protein functions

Research hypothesis

We hypothesized that a proportion of SLE patients had an elevated level of DcR3, some others had gain-of-function mutations of the *DcR3* gene leading to an increased activity of the protein, in spite of its normal amount.

Expected benefits

This is the first study to determine the level of DcR3 serum of juvenile SLE patients. We provide significant findings that serum DcR3 was elevated in active SLE in comparison to inactive SLE and unaffected controls. We expect that DcR3 would be a new biomarker for SLE diagnosis, and the level of serum DcR3 could be used to indicate the activity of disease. Most importantly, we, for the first time, identified mutations in the *DcR3* gene that significantly enhanced lymphocyte proliferation *in vitro*. This strongly suggests their etiologic roles in SLE pathogenesis. We hope that our results could provide further insight into the pathogenesis of SLE which is a multi-factorial disorder and its etiology remains unclear.

Conceptual Framework

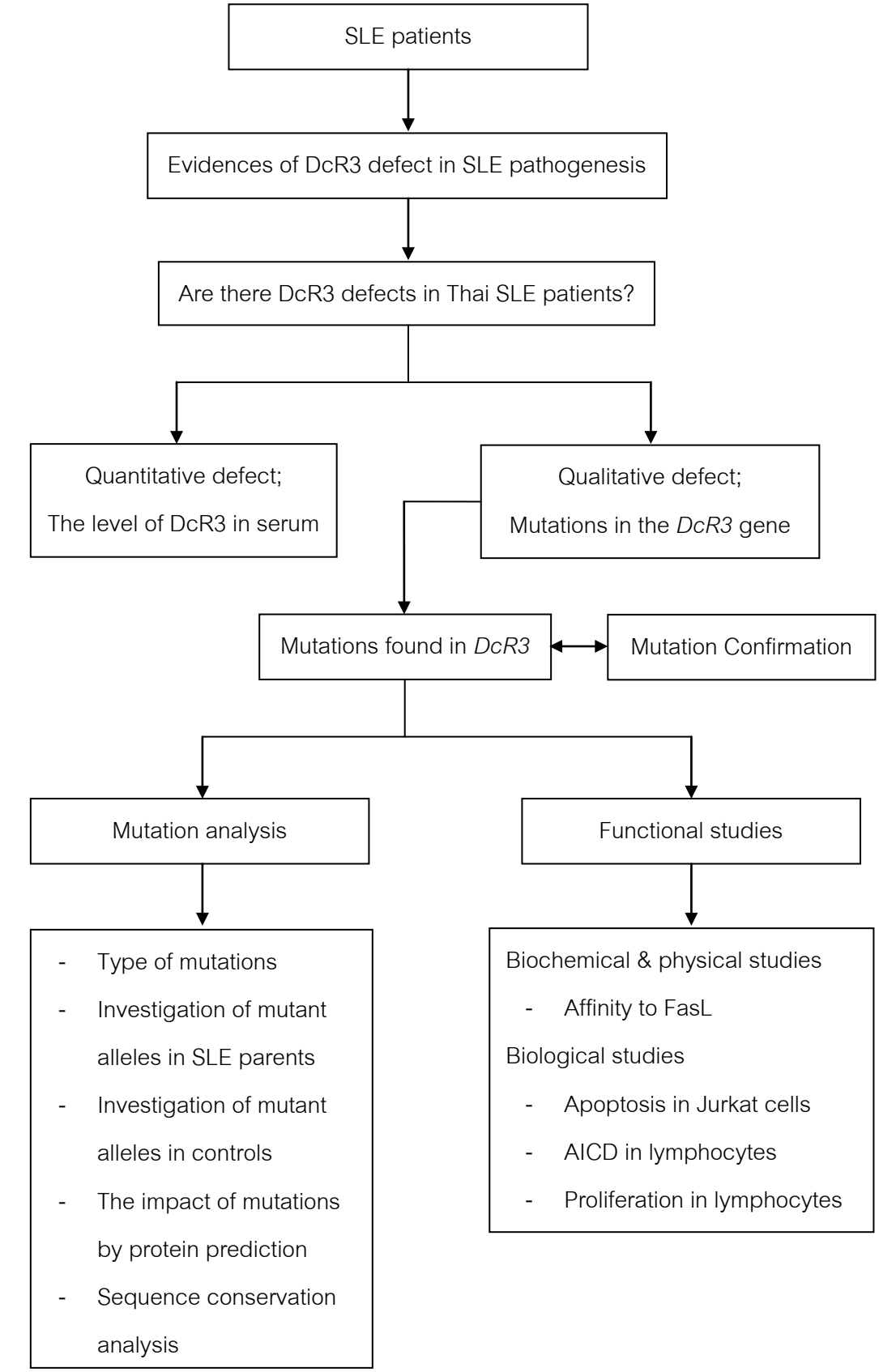

Research methodology

We determined whether there were defects in DcR3 in SLE patients including quantitative and qualitative defects.

For quantitative defect, we measured the level of serum DcR3 in juvenile SLE patients and aged-matched unaffected controls by ELISA.

For the qualitative defect, we identified whether there were mutations in the *DcR3* gene and their effect on protein function. We screened the mutations in the *DcR3* gene in 200 SLE patients including 100 of juvenile and adult SLE patients.

The mutations in the *DcR3* gene were analyzed whether they affected the protein functions by PolyPhen and SIFT programs. The type of mutations was classified and the mutations were confirmed by PCR-RFLP. Then the mutant alleles were investigated in SLE parents to show whether the mutations were inherited or *de novo*. In addition, we did DcR3 orthologue comparison among vertebrate species to determine whether the mutation locations were evolutionarily conserved. The mutant alleles were explored in ethnic-matched unaffected controls to show whether the mutations were present in the general population.

To study whether the mutations affected the protein functions, the wild type and mutant proteins were produced using mammalian cell lines. Briefly, we obtained the *DcR3* expression vector from Gene Tech, USA and then we did site-directed mutagenesis to construct mutant *DcR3* expression vectors. Both the wild type and mutant *DcR3* expression vectors were transfected into COS7 to produce wild type and mutant protein. Because DcR3 is a secreted protein, we purified the proteins from the cultured supernatant. We used affinity chromatography to purify the proteins. Then the purified proteins were examined by Western blot and Coomassie blue staining and used for protein functional analyses.

For the protein functional studies, we determined whether the mutations affected the protein affinity to FasL. their affect on biological functions was evaluated by studying the role of mutations in FasL-induced Jurkat cell apoptosis, activation induced cell death (AICD) in lymphocytes and lymphocyte proliferation.

CHAPTER II

LITERATURE REVIEW

General concept of SLE

Systemic Lupus Erythematosus (SLE) is an autoimmune disease which has autoantibody production and affects multiple organs in the body. The disease shows clinical heterogeneity according to 11 criteria established by American College of Rheumatology as shown in table 1 with 4 clinical characteristics requirement for SLE diagnosis [6]. The prevalence of the disease ranges from 7.4 – 159.4 per 100,000 worldwide [1]. The prevalence is higher among the Asian, African American, African Caribbean, and Hispanic American than in the Caucasian [26]. In juvenile SLE, the sex ratio is quite not different. The children younger than two years old have even SLE occurring in both male and female and the ratio alters to 4:3 during the first decade of their life [2]. In adult SLE, the disease affects female greater than male with the ratio of 9:1 and the ratio changes to 5:1 after the age of 50 years [3-5].

Table 1. American College of Rheumatology Criteria for the Diagnosis of SLE [6]

Malar rash	A rash on the cheeks and nose, often in the shape of a butterfly
Discoid rash	A rash that appears as red, raised, disk-shaped patches
Photosensitivity	A reaction to sunlight that causes a rash to appear or get worse
Oral ulcers	Sores in the mouth
Arthritis	Joint pain and swelling of two or more joints
Serositis	Inflammation of the lining around the lungs (pleuritis) or inflammation of the lining round the heart that causes chest pain, which is worse with deep breathing (pericarditis)
Kidney disorder	Persistent protein or cellular casts in the urine

Neurologic disorder	Seizures or psychosis
Blood disorder	Anemia (low red-cell count), leukopenia (low whitecell count), lymphopenia (low level of specific white cells), or thrombocytopenia (low platelet count)
Immunologic disorder	Positive test for anti–double-stranded DNA, anti-Sm, or antiphospholipid antibodies
Abnormal antinuclear antibodies	Positive antinuclear-antibody test

Etiology of SLE

The etiology of SLE is not clearly established. However, there are four major factors contributing to SLE pathogenesis consisting of genetics, environment, hormone, and epigenetic regulation [6].

Genetic is a crucial factor contributing to SLE supported by a high sibling risk ratio (λ_s), with λ_s= 8 – 29 [27], and higher concordance rates between monozygotic twins relative to dizygotic twins, with >24-58% and >2-5% respectively [14]. In addition, the disease exhibits familial clustering, with 10% to 12% of SLE patients having an affected first-degree relative [13]. The genetic variations in SLE were first revealed to be an important factor in SLE in human leukocyte antigen (HLA) region which contains a group of genes responsible for immune function. So far, more than 56 genes are now elucidated to contribute individuals to SLE [6]. Recently, SLE has been shown to be Mendelian mode of inheritance in six families in Arabian. They found homozygous 1-bp deletion in *DNASE1L3* leading to loss of enzymatic function of protein and impairment of degraded DNA clearance in SLE [28]. Another interesting gene associated with SLE is *TREX1* which its function resembles to *DNASE1L3*. They found two heterozygous frameshift mutations in *TREX1* in UK and German SLE patients and the mutant alleles alter the proteins sub cellular targeting implicating in SLE

pathogenesis [29]. Although some cases in SLE are associated with the malfunction of single gene, the disease mostly arise from the effect of combination genes variants[6]. The most SLE associated SNPs has been found in non-coding regions of immune response related genes [30]. In addition to DNA variants associated with SLE, the copy number variation of some genes, for example *C4*, *FCGR3B*, and *TLR7*, has been linked to disease activity [31-33]. Although many SNPs have been found to associate with SLE, but some SNPs that are associated with SLE in Caucasians but they are not found to associate with SLE in Asians, for example *PTPN22* and *LYN* [34-36]. In addition, *ITGAM* has also been found to be SNPs associated with SLE in European, African and Hispanic American; however, this association study shows no significance in Asian population [27, 37-39].This shows that SLE is multifactorial disease which not only genetic factors but also other factors can cause the disease.

As for environmental factors, sunlight is the most obvious environmental factor that aggravate the disease [1]. Other factors have been considered, for examples, crystalline silica and mercury was postulated as a risk for development of SLE. In addition, some drugs were reported as an agent-induced SLE, for example, procainamide, hydralazine, quinidine, and phenytoin. Furthermore, Epstein-Barr virus (EBV) has also been identified as a possible factor that leads to development of lupus [13]. Paradoxically, ninety percent of the adult population are infected with EBV; however, the prevalence of SLE still remains very low [1], which indicates that SLE is a multifactorial disease.

Hormonal status has been considered as one important factor in SLE. The disease affects women of childbearing age and exogenous estrogen exacerbates lupus or increase the risk of SLE development. In mouse model, a bias towards the disease in one sex is normalized in both male and female by castration or administration of estrogen to males. Furthermore, the hormone replacement therapy (HRT) was associated with an increased risk of SLE [40, 41].

Epigenetic is also postulated to be a factor contributing to SLE. In animal model, lupus prone mice (MRL-*lpr/lpr*) had H3 and H4 histone hypoacetylation in

spleenocytes [42]. In addition, the lupus prone mice administered with histone deacetylase inhibitors recover from glomerulonephritis and splenomegaly [43]. There are some genes that are associated to SLE pathogenesis, for example *ITGAL*, *CD40LG*, *CD70* and *PPP2CA*and those are hypomethylation in SLE[6]. Epigenetic could also be linked to the environmental factor because some drugs, for example hydralazine and procainamide, affect DNA methylation and can induce SLE in healthy persons [44].

DcR3 in SLE pathogenesis

The defect in apoptotic pathway has been postulated to contribute to SLE pathogenesis [45]. For example, mutations in *Fas* and *FasL* are found in SLE and autoimmune lymphoproliferative syndrome (ALPS) patients [46-49]. In murine models, *lpr*/*lpr* and *gld*/*gld* mice which have mutations in *Fas* and *FasL* developed autoimmune disease [50-52]. Fas and FasL play a role in peripheral T cell apoptosis which is an important mechanism for peripheral tolerance and the breakdown of this mechanism is thought to be a causation of autoimmunity [49, 53]. Briefly, this mechanism is called activation induced cell death (AICD) which is the process to maintain tolerance of T cell to self-antigen [49, 54]. Activation induced cell death is apoptotic process induced by repeated stimulation of T cell receptor and then the apoptosis is occurred by the ligation of FasL to Fas receptor on the T cell surface triggering caspase cascade then initiating T cell apoptosis [53]. In addition, mutations in both genes were reported as a pathogenic causation in SLE [22, 23]. However, mutations in *Fas* or *FasL* in SLE are rare. Therefore, the defect in apoptosis pathway triggered by Fas and FasL interaction might be involved by other molecules. In 1998, there was a report that a molecule called DcR3 can compete with Fas receptor to bind to Fas ligand and suppress apoptosis in FasL-induced apoptosis in Jurkat cells and AICD in T cell [55]. In 2007, There was a study showing that overexpression of human *DcR3* in mice resulted in SLE-like syndrome as shown in figure 1 [16]. In addition, there were two studies reporting that serum *DcR3* was elevated in SLE patients [17, 19]. These studies showed that the level of DcR3 in serum was significantly elevated in SLE patients in comparison to healthy

controls. They also investigated the role of DcR3 in T cell apoptosis and exhibited DcR3 induced apoptosis suppression in T cell and enhanced T cell proliferation. They concluded that DcR3 possibly played a pathogenic role in SLE via reduction in apoptosis and enhancing activation of T cell [19]. Although, there were elevated serum DcR3 levels in SLE patients, there were undetectable serum DcR3 in some SLE patients. Hence, the defect in DcR3 in SLE might not only be resulted from quantitative defect, but there might also be a qualitative defect such as mutations in the *DcR3* gene playing a pathogenic role in SLE.

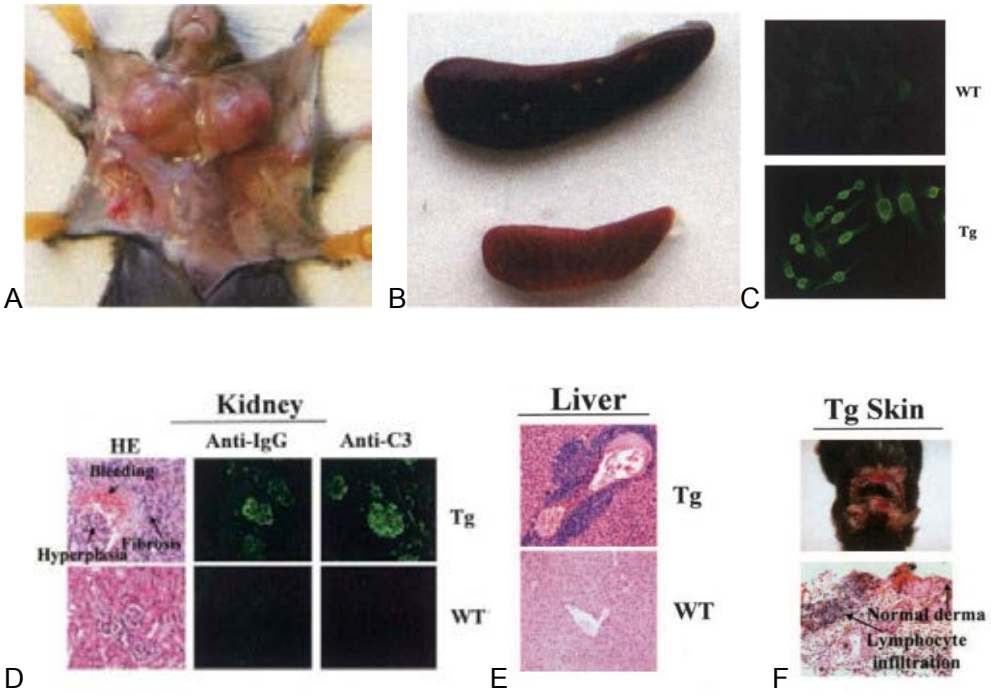

Figure 1. SLE-like syndrome in human *DcR3*-transgenic mice (A) Lymphadenopathy (B) Spleen enlargement (C) Presence of antinuclear antibody (D) Renal histopathology: glomeruli enlargement, interstitial fibrosis and deposition of IgG and C3 (E) Liver lymphocyte infiltration (F) Derma lymphocyte infiltration [16]

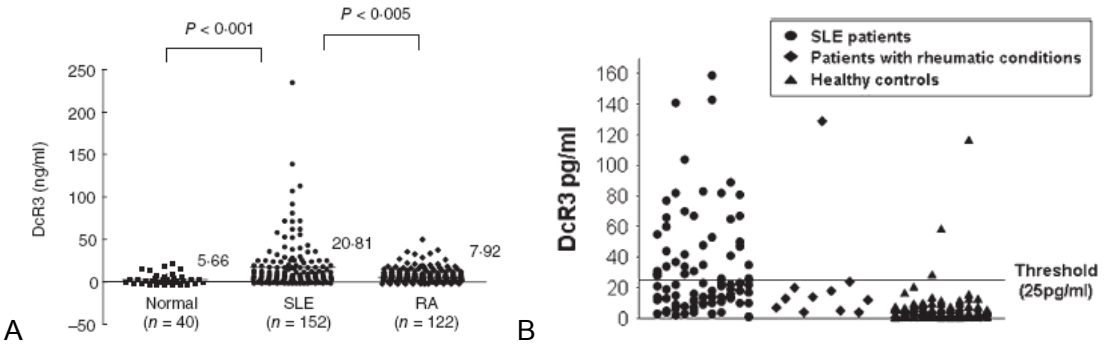

Figure 2. Elevation of serum DcR3 in SLE patients in comparison to RA patients and healthy controls; (A) Taiwanese population [19] (B) Mexican population [17]

Biological functions of DcR3

Human *DcR3* was discovered in 1998 and it is a member of tumor necrosis factor receptor (TNFR) superfamily [55]. The protein in this family commonly shares cysteine-rich repeats in the molecule [56]. According to NCBI database (NC_000020.10, Gene ID: 8771), *DcR3* is a gene on chromosome 20 q13.3 and it officially names tumor necrosis factor receptor superfamily member 6b (TNFRSF6B). Transcript of *DcR3* (NM_003823.3) is 1,155 bp consisting of 3 exons which produce 300 amino acid residues (NP_003814.1). Unlike other members in TNFR family, DcR3 lacks of transmembrane protein sequence; therefore it is a secreted protein [55, 56]. DcR3 is identified to be a decoy receptor for FasL, LIGHT, and TL1A [55-57]. FasL induces T cell apoptosis by signaling through Fas receptor [58]. Blocking of FasL signaling by DcR3 might activate overactive immune response and contribute to autoimmune diseases development [59, 60]. DcR3 is highly expressed in tumor cells and it is thought that tumor cells might escape cytotoxic immune cells attack by expressing DcR3 and blocking FasL-induced tumor cells apoptosis [55, 61]. LIGHT signaled through HVEM receptor on T cell triggered T cell proliferation [62]. Blockage in LIGHT signaling by DcR3 reduced T cell activity *in vitro* and graft-versus-host responses *in vivo* [63]. TL1A expressed on antigen presenting cells also promoted T cell proliferation, but through DR3 receptor on activated T cell [57, 64]. Inhibition of TL1A signaling by DcR3 has been

proposed to be an approach for autoimmune disease treatment [65]. In addition, TL1A acts as an autocrine molecule secreted from endothelial cell and induce apoptosis itself. Blocking of TL1A by DcR3 promoted neovascularization and tumor growth [66].

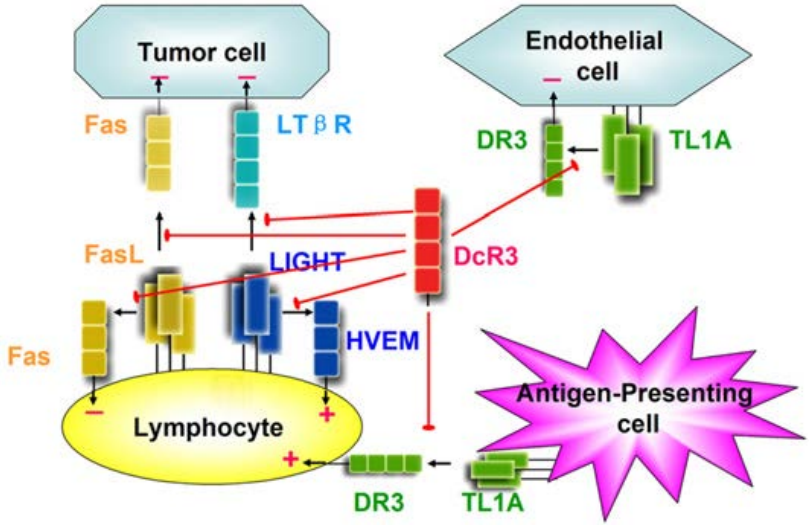

Figure 3. DcR3 and its ligands; FasL (yellow), LIGHT (blue) and TL1A (TL1A (green); Soluble DcR3 binds to these ligands and blocks their signal transduction pathways. FasL induces lymphocyte and tumor cell apoptosis (-). LIGHT trigger lymphocyte proliferation (+). TL1A induces apoptosis (-) in endothelial cell and triggers lymphocyte proliferation (+) [67].

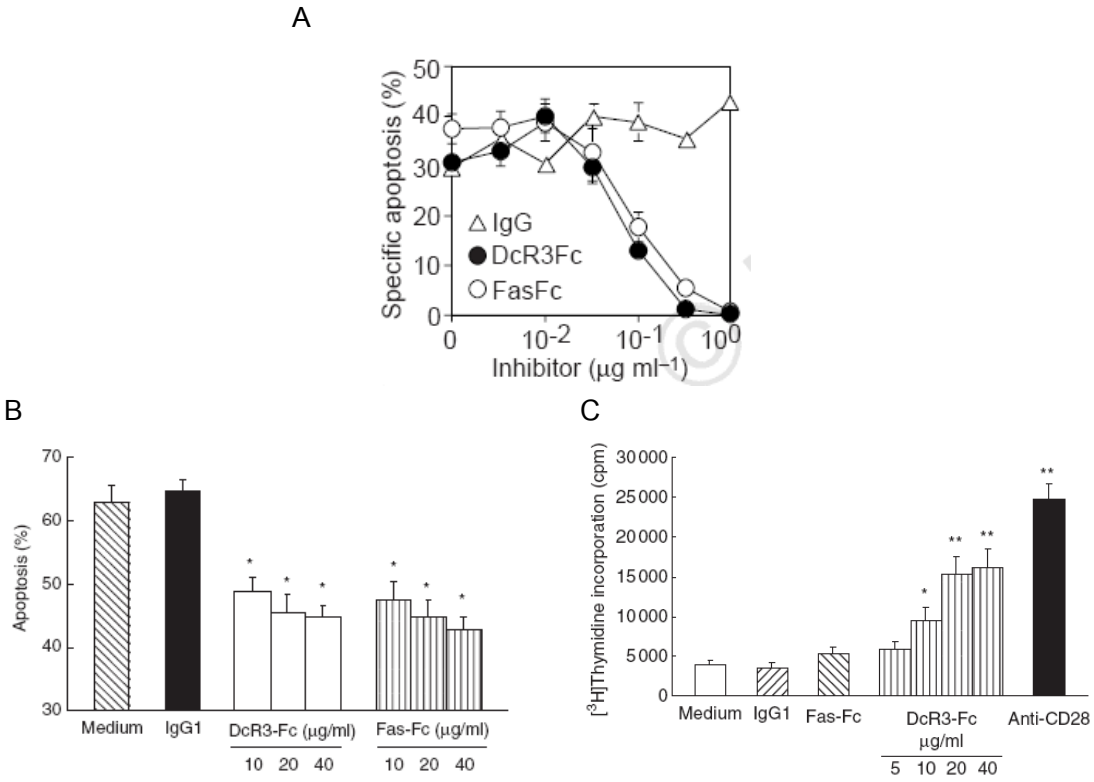

Figure 4. Biological function studies of DcR3; (A) DcR3 inhibited FasL-induced apoptosis in Jurkat cell; Jurkat cell were treated with FasL to induce apoptosis in the presence or absence of DcR3-Fc, Fas-Fc and IgG. DcR3 inhibited FasL-induced Jurkat cells apoptosis as well as Fas-Fc in dose dependent manner [55]. (B) DcR3 suppressed activation induced cell death (AICD) in T cells; Human T cells were stimulated with PHA and re-stimulated with anti-CD3 in the presence of IL-2 to induce activation induced cell death (AICD) process in the presence or absence of DcR3-Fc, Fas-Fc, and IgG1. DcR3 inhibited AICD in T cells as well as Fas-Fc in dose dependent manner[19]. (C) DcR3 enhanced T-cell proliferation in conjunction with signals through T cell receptor; Human T cells were cultured in suboptimal concentration of anti-CD3 in the presence or absence of DcR3-Fc, Fas-Fc, anti-CD28, and IgG1. DcR3 induced co-stimulation of human T cells as well as anti-CD28, but not Fas-Fc [19].

DcR3 structure and affinity to its ligands

There is a study showing affinity between DcR3 and its ligands (figure 5). DcR3 binds to TL1A, LIGHT and FasL with different affinities determined by SPR technique. The affinity of DcR3 to LIGHT is approximately 4 and 20 folds higher than TL1A and FasL respectively. There is only a modeling structure of DcR3 and TL1A interaction (figure 6). It indicated that DcR3 used cysteine-rich domain 2 (CRD2) to recognize TL1A molecule. In addition, the study exhibited L85A/R89A double mutant DcR3 exhibited lower affinity not only to TL1A but also LIGHT and FasL as well. It might be likely that LIGHT and FasL share the same binding site in DcR3 similar to TL1A [67].

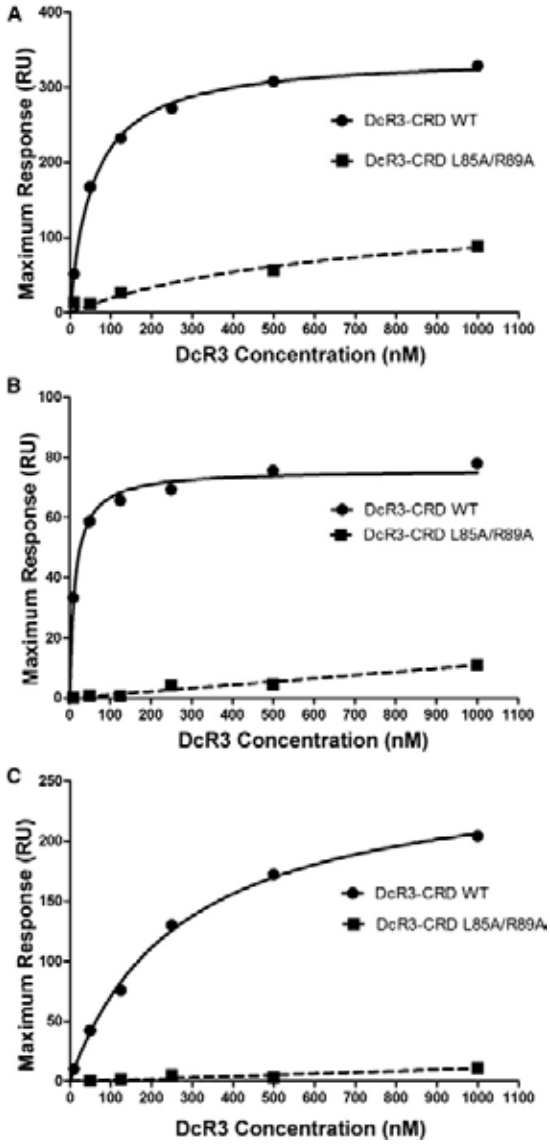

Figure 5. The binding affinities of DcR3and its ligands; The affinities of wild type DcR3 cysteine-rich domains (V30-S195, solid line) and L85A/R89A DcR3 double mutant (dash line)to immobilized (A) TL1A, (B) LIGHT and (C) FasL by SPR technique; Wild typeDcR3 cysteine-rich domains bind to TL1A, LIGHT and FasL with the Kd of 56.4 ± 3.7, 14.0 ± 2.0, and 271.4 ± 24.4 nM, respectively while the L85A/R89A DcR3 double mutant showed significantly lower binding response to each ligand [67].

A

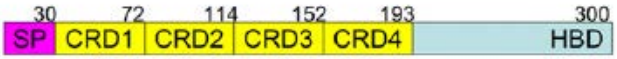

B

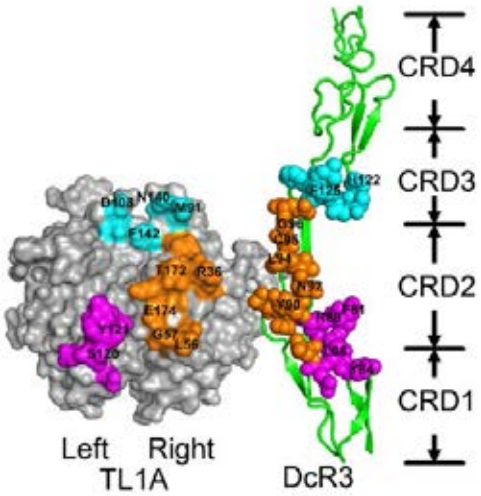

Figure 6. DcR3 domains structure and interaction interface with TL1A (A) DcR3 domains structure; DcR3 consists of a signal peptide (SP), four cysteine-rich domains (CRD) and heparan-binding domains (HBD). The number indicates the last amino acid residue in each domain. (B) Interaction interface between TL1A and DcR3; cysteine-rich domain 2 (CRD2) in DcR3 recognizes TL1A molecule.

CHAPTER III

METHODOLOGY

Quantification of serum DcR3 by ELISAs

Serum DcR3 of SLE patients and unaffected controls were measured using an ELISA kit (BMS2031, Bender MedSystems®, Vienna, Austria) according to the protocol of manufacturer. The unaffected controls recruited in this experiment were not autoimmune and cancer patients because DcR3 was reported to be overexpressed in these diseases. The absorbance was measured at 450 nm using BiotrakII Plate Reader (Biosciences, Amersham, Sweden). For comparison of serum DcR3 between each group, unaffected controls, inactive and active SLE patients, the Mann-Whitney U test was used for statistical analysis. Graphs and statistical analyses were conducted by GraphPad Prism 5.0 software. The *p*-value less than 0.05 was considered as statistical significance.

DcR3 sequencing in SLE patients

Peripheral blood samples were collected from the patients and their available parents after written informed consents were obtained. SLE patients' and unaffected controls' genomic DNA were extracted from peripheral blood using Qiagen DNA extraction kits according to manufacturer's instructions (Qiagen, Valencia, CA, USA). PCR amplification reactions of the entire coding regions were carried out in a 20 µl volume containing 50 ng genomic DNA, 1X PCR buffer, 1.5 mM $MgCl_2$, 0.2 mM dNTPs, 0.2 mM of each primers as shown in table 1, 5% DMSO and 0.5 U *Taq* polymerase, using the following parameters: initial denaturation at 94^{O}C for 3 minutes, 35 cycles of 30 seconds at 94°C, 45 seconds at the appropriate annealing temperature and extension time as shown in table 1 at 72°C, and 10 minutes at 72^{O}C final extension. PCR products were treated with ExoSAP-IT according to the manufacturer's

recommendations (USP Corporation, Cleveland, OH, USA), and sent for direct sequencing (Macrogen Inc., Seoul, Korea).

Table 2. Primers and PCR conditions for mutation screening in the *DcR3* gene

Exon	Primers	Annealing Temp. (^{O}C)	Extension Time (min'/sec")	PCR size (bp)
1 – 2	Forward 5'CACCCTTGGACTGAGCTCT3' Reverse 5'GGCATGCCTCAGGCTAGATG3'	64	1' 20''	1,112
3	Forward 5'AGCTCTCTGACCGAAGGCTC3' Reverse 5'CCTCTTTCAGTGCAAGTGGG3'	60	45"	536

RFLP of mutant alleles in controls

The mutations found in *DcR3* were explored in 500 normal controls by RFLP. Genomic DNA was extracted from peripheral blood of unaffected ethic-matched controls using Qiagen DNA extraction kits according to manufacturer's instructions (Qiagen, Valencia, CA, USA). PCR amplification covering nucleotide 167 and 364 according to the transcription start site of *DcR3* were carried out in a 20 µl volume containing 50 ng genomic DNA, 1X PCR buffer, 1.5 mM $MgCl_2$, 0.2 mM dNTPs, 0.2 mM of each primers as shown in table 2, and 0.5 U *Taq* polymerase, using the following parameters: initial denaturation at 94^{O}C for 3 minutes, 35 cycles of 30 seconds at 94°C, 30 seconds at the appropriate annealing temperature as shown in table 2, and 30 seconds at 72°C. RFLP analysis was performed in 20 µl of each the respective PCR products by subjecting them to the following restriction enzymes (New England Biolabs® Inc.) at a 10U concentration: *Ban*I for c.C167T and *Rsa*I for c.C364T with overnight incubation at 37°C and 30 minutes heat inactivation at 65^{O}C. The resulting products were further analyzed by 2% agarose gel electrophoresis.

Table 3. Primers and PCR conditions for PCR-RFLP in mutant allele investigation

Mutation/ Restriction enzyme	Primers	Annealing Temp. (^{O}C)	PCR size (bp)	Types of analysis
c.C167T/ *Ban*I	Forward 5' AGTGGCAGAAACACCCACCTACC 3' Reverse 5' AGGTGGACACGATGCGTGCTCC 3'	60	316	Wild type cut
c.C364T/ *Rsa*I	Forward 5'GAGTGGCAGAAACACCCACC3' Reverse 5'AACTGGTGTCCTAGCTCAGG3'	63	443	Mutant cut

DcR3 sequence analysis and prediction of impact of mutations

For protein sequence comparison, *DcR3* orthologues were obtained by searching the *TNFRSF6B* gene in all species available from Ensembl website (http://www.ensembl.org/index.html). The DcR3 protein sequences from 14 vertebrate species including *Gallus gallus* (Chicken), *Meleagris gallopavo* (Turkey), *Taeniopygia guttata* (Zebra finch), *Homo sapiens* (Human), *Ailuropoda melanoleuca* (Panda), *Bostaurus* (Cow), *Loxodonta africana* (Elephant), *Myotis lucifugus* (Little brown bat), *Sarcophilus harrisii* (Tasmanian devil), *Anolis carolinensis* (Anole lizard), *Ornithorhynchus anatinus* (Platypus), *Takifugu rubripes* (Puffer fish), *Tetraodon nigroviridis* (Green spotted puffer fish) and *Gadus morhua* (Alantic cod) were aligned by ClustalX2 software (version 2.0.11). PolyPhen (http://genetics.bwh.harvard.edu/pph/) and SIFT (http://sift.jcvi.org/www/SIFT_enst_submit.html) online software were used to predict the possible impact of both missense mutations on the protein function.

Wild type and mutant DcR3 expression vector construction

The pRK5-*DcR3-Fc* expression vector was given by Genetech, San Francisco. The vector contains coding regions of *DcR3* fused with *Fc* region of human *IgG1*. Two mutations, consisting of c.C167T and c.C364T, were introduced into pRK5-DcR3-IgG1 by QuikChange® Lighting Site-Directed Mutagenesis Kit according to the

manufacturer's instruction (Stratagene, California). The vectors were transformed into *Escherichia coli DH5α* according to a laboratory manual, Molecular Cloning, Sambrook and Russell. The vectors were extracted from the transformed *E. coli* by QIAGEN® Plasmid Mini Kit according to the manufacturer's instruction (Qiagen). The wild type, c.C167T, and c.C364T *DcR3-Fc* were subsequently sub-cloned to the pIRES2-EGFP expression vector.

Transfection

For SPR experiment, COS7 cell lines were transiently transfected with the wild type, c.C167T, and c.C364T pRK5-*DcR3-Fc* expression vectors by Lipofectamine™2000 reagent according to the manufacturer's instruction (Invitrogen). For apoptosis and proliferation assay, COS1 or Cos7 cell line was transiently transfected with the wild type, c.C167T, and c.C364T pIRES2-*EGFP-DcR3-Fc* expression vectors by Lipofectamine™2000 reagent according to the manufacturer's instruction (Invitrogen). Plasmid and Lipofectamine™2000 ratio is 1 to 2.5. The expression of transgenes was examined by Western blot and Flow cytometry (Guava EasyCyte Plus, Millipore).

Protein expression analysis

Expressed wild type, p.T56I, and p.H122Y DcR3-Fc were examined in cell culture supernatant and cell lysates by Western blot. The total protein concentration of cell culture supernatant and cell lysates was measured using Micro BCA™ Protein Assay according to manufacturer's instruction (Thermo Scientific). Proteins in supernatant and cell lysates were separated by 12 % SDS-PAGE and transferred onto PVDF membranes using iBlot® Dry Blotting System (Invitrogen). The membranes were blocked with 5% non-fat dry milk for 1 hour and incubated with 0.2 µg/ml anti-human DcR3 antibody (goat IgG, AF142, R&D System). The membranes were washed with TBS-T and incubated with 0.1µg/ml goat IgG horseradish peroxidase conjugated antibody (rabbit IgG, HAF017, R&D System) for 1 hour. The membranes were washed and incubated with SuperSignal West Pico Chemiluminescent Substrate according to

the manufacturers' instructions (Thermo Scientific). Bound antibodies were visualized by ImageQuant LAS 4000 (GE-Healthcare).

Protein purification

Cell culture supernatant were dialyzed against binding buffer (20 mM sodium phosphate, pH7.0) and applied to HiTrap™ Protein G HP Columns (GE Healthcare). After washing the column with binding buffer, the bound proteins were eluted with elution buffer (100 mM Glycine-HCl buffer, pH2.7). In addition, each fraction was neutralized with 1.0 M Tris-HCl, pH9.0 to preserve protein stability. The purified fractions were dialyzed against phosphate buffered saline (PBS), then the protein concentration was measured using Micro BCA™ Protein Assay according to manufacturer's instruction (Thermo Scientific) and the proteins were used in further downstream functional analysis experiments.

Protein biding and affinity assay

To determine binding affinities between FasL versus wild type, p.T56I and p.H122Y DcR3-Fc, we did Surface Plasmon Resonance (SPR) spectroscopy (Autolab Esprit®, Eco Chemie, The Netherlands). Affinity and kinetic analyses were performed at 25^{O}C in PBS. Fifty micro liters of FasL (10 µg/ml) in PBS were directly immobilized to 50%surface grafted poly(acrylic acid) sensor chip [68] by amine coupling reaction by incubating the sensor chip with 10 mM sodium acetate buffer pH 4.5 for 150 seconds then activating carboxyl groups in the sensor chip with 0.1 M EDC and 0.1 M NHS for 5 minutes, resulting in immobilization levels of 119 – 138.3 millidegrees corresponding to 99.2 – 115.3 ng/cm^2 (a change of 120 millidegrees corresponds to 100 ng/cm^2 binding). Doubling dilutions, ranging from 346 to 10.8 nM of wild type, p.T56I and p.H122Y DcR3-Fc were injected to immobilized FasL sensor chip (association step) for 5 minutes then PBS was injected to the sensor chip to wash the unbound proteins for five minutes (dissociation step). The binding between immobilized FasL and DcR3 was removed by injection of 10 mM Glycine-HCl pH 2.3 for 5 minutes

twice (Regeneration) then the sensor chip was equilibrated with PBS until restoring the baseline signal and used for next binding assay. The protein binding constants were evaluated by using Kinetic Evaluation version 5.3 software (Autolab Esprit®, Eco Chemie, The Netherlands) assuming the monophasic association model. The binding model equation is $Y = \frac{B_{max}X}{(K_d + X)}$, where B_{max} = is the maximum specific binding and K_d is the equilibrium binding constant.

Apoptosis assay in Jurkat cells

Apoptosis in Jurkat cell was induced by FasL induction. Cells were cultured in RPMI-1640 supplemented with 10% fetal bovine serum (FBS) and antibiotics (Penicillin/Streptomycin) and treated with 7.27 ng/ml FasL-FLAG cross linked with 0.25 µg/ml anti-FLAG in the absence or presence of wild type, p.T56I and p.H122Y DcR3-Fc at 37^{O}C for 16 hours. Jurkat cell apoptosis was determined by AnnexinV/Propidium iodide staining after 16 hours DcR3 and Fc treatment. For lymphocytes apoptosis assay, cells were centrifuged and wash with PBS and then resuspended in 200 ul of AnnexinV binding buffer (25 mM HEPES, 140 mM NaCl, 1 mM EDTA, pH 7.4, 0.1% bovine serum albumin). One micro liter of Alexa Fluor® 488 AnnexinV (V13241, Invitrogen) was then added to each sample and the samples were incubated at room temperature in the dark for 15 minutes. One micro liter of 100 µg/ml PI was added to each sample and then analyzed by flow cytometry (Guava EasyCyte Plus, Millipore). The experiment was performed three times. Statistical analyses were evaluated by Student's *t*-test and *p*-value less than 0.05 was considered as statically significant.

Activation-induced cell death (AICD) in lymphocytes

Lymphocytes were isolated from peripheral blood using Lymphoprep™ (AXIS-SHELD). The lymphocytes were stimulated with 1 µg/ml phytohaemagglutinin (PHA) for 24 hours and cultured in the presence of 1 ng/ml interleukin-2 (IL-2) for 5 days at 37^{O}C in RPMI-1640 supplemented with 10% fetal bovine

serum (FBS) and antibiotics (Penicillin/Streptomycin). The activated lymphocytes were then re-stimulated with plate-bound anti-CD3 (1 µg/ml anti-CD3 in PBS during plate coating, MAB100, R&D system) in the absence or presence of wild type, p.T56I and p.H122Y DcR3-Fc (0 – 20 µg/ml) and human Fc (10 µg/ml) as a control on day 7. Lymphocytes apoptosis was then determined by AnnexinV/Propidium iodide staining after 16 hours. For lymphocytes apoptosis assay, cells were centrifuged and wash with PBS and then resuspended in 200 ul of AnnexinV binding buffer (25 mM HEPES, 140 mM NaCl, 1 mM EDTA, pH 7.4, 0.1% bovine serum albumin). One micro liter of Alexa Fluor® 488 AnnexinV (V13241, Invitrogen) was then added to each sample and the samples were incubated at room temperature in the dark for 15 minutes. One micro liter of 100 µg/ml PI was added to each sample and then analyzed by flow cytometry (Guava EasyCyte Plus, Millipore).The samples were obtained from 5 different healthy controls. Statistical analyses were evaluated by Student's *t*-test and *p*-value less than 0.05 was considered as statically significant.

Proliferation in lymphocytes

Lymphocytes were isolated from peripheral blood using Lymphoprep™ (AXIS-SHELD). The cells ($2x10^5$ cells/well) were cultured for 72 in 96-well pre-coated with sub-optimal anti-CD3 concentration (50ng/ml anti-CD3 in PBS during plate coating, MAB100, R&D system) in the presence or absence of wild type and p.T56I and p.H122Y DcR3-Fc. Human Fc (10 µg/ml) and anti-CD28(1 µg/ml) were used as controls for the experiment. After 72 hours incubation, the cultures were pulsed with [^{3}H]-thymidine (1.0 uCi/well) for 16 hours before cell harvesting. Then [^{3}H]-thymidine incorporation was measured by Multipurpose Scintillation Counter (LS6500, Beckman). The samples were obtained from 4 healthy controls and performed as triplicate. The value which was the most distant from mean was considered as outliers and excluded from the statistical analysis. Statistical analyses were evaluated by Student *t*-test and the *p*-value less than 0.05 was considered as statistically significant.

CHAPTER IV

RESEARCH RESULTS

The level of serum DcR3 in juvenile SLE patients

There were several studies revealing that the level of serum DcR3 was elevated in SLE patients in comparison to healthy controls and DcR3 might play a pathogenic role in SLE [17, 19, 69]. We measured serum DcR3 in juvenile SLE patients (n = 61) and unaffected controls (n = 28). Means of serum DcR3 of juvenile SLE patients and unaffected controls were 181.7 and 65.52 pg/ml respectively. Although difference of means of serum DcR3 between juvenile SLE patients and unaffected controls was 116.18 pg/ml, it was not significantly different (p = 0.219). Interestingly, when we set the threshold serum DcR3 concentration at 200 pg/ml, there were only 3.6% of controls with positive serum DcR3 (n = 1/28); whereas juvenile SLE patients were 31.2% DcR3 positive (n = 19/61). Then we investigated whether the level of serum DcR3 correlated with SLE disease activity by analyzing the level of serum DcR3 in patients with active and inactive disease. The means of serum DcR3 in inactive and active disease were 118.4 and 440.2 pg/ml, respectively. Patients with active SLE have significantly elevated levels of serum DcR3 in comparison to those in the inactive SLE patients (p = 0.003) and unaffected controls (p=0.001). However, it was not significantly different between serum DcR3 of inactive SLE patients and unaffected controls (p = 0.763). .According to threshold level of DcR3 at 200 pg/ml, it was 66.7% DcR3 positive (n = 8/12) which was the highest proportion among three groups; whereas inactive SLE and controls had 22.5% (n = 11/49) and 3.6% (n = 1/28) DcR3 positive, respectively.

As for the serum DcR3 of SLE patients with mutations in the *DcR3* gene, the adult SLE patient during inactive state and her mother had undetectable serum DcR3 while the juvenile SLE patient during inactive state had serum DcR3 of 172.55 pg/ml.

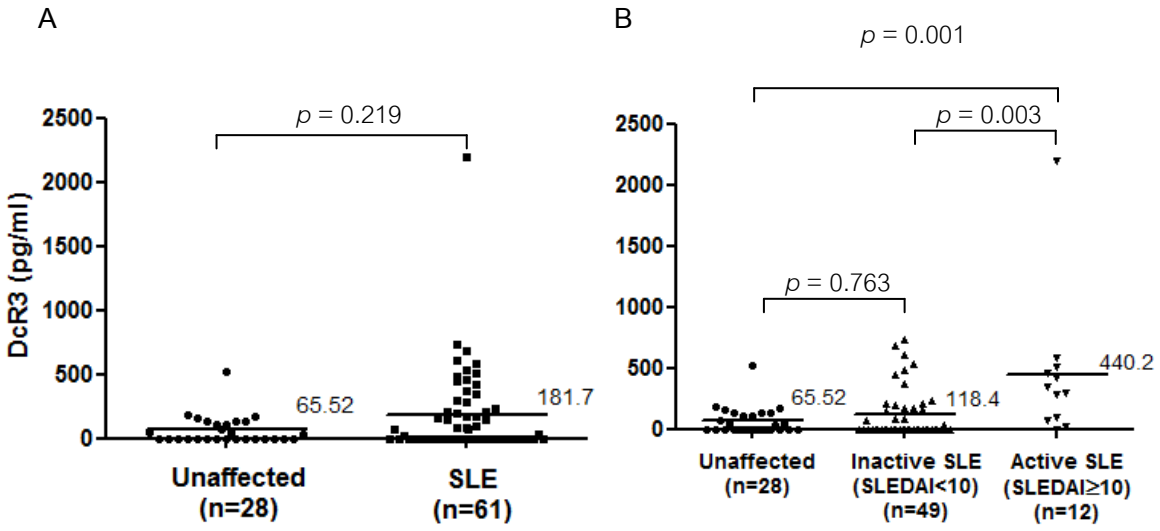

Figure 7. The level of serum DcR3 in unaffected controls, inactive, and active SLE patients; (A) Serum DcR3 concentrations in 61 juvenile SLE patients and 28 age-matched unaffected controls (B) Serum DcR3 concentrations in SLE with active [SLE disease activity index (SLEDAI) ≥ 10; n=12] and inactive SLE [SLE disease activity index (SLEDAI) <10; n=49]; Horizontal line showing the mean of serum DcR3 as the number indicated; Statistics analyzed by the Mann-Whitney U rank sum test; *p*-value<0.05 was considered as statistically significant. The serum DcR3 levels of the adult SLE patient with mutation and her mother were excluded from the statistical analysis.

Identification of mutations in *DcR3* in SLE patients

We sequenced entire coding regions of the *DcR3* gene in 200 SLE patients. There were two mutations in exon 1 of the *DcR3* gene in two unrelated SLE patients. Two mutations were heterozygous c.C167T and c.C364T according to the *DcR3* translation start site. Both of them are missense mutations which result in amino acid substitutions. Then, both mutations were confirmed by PCR-RFLP.

A

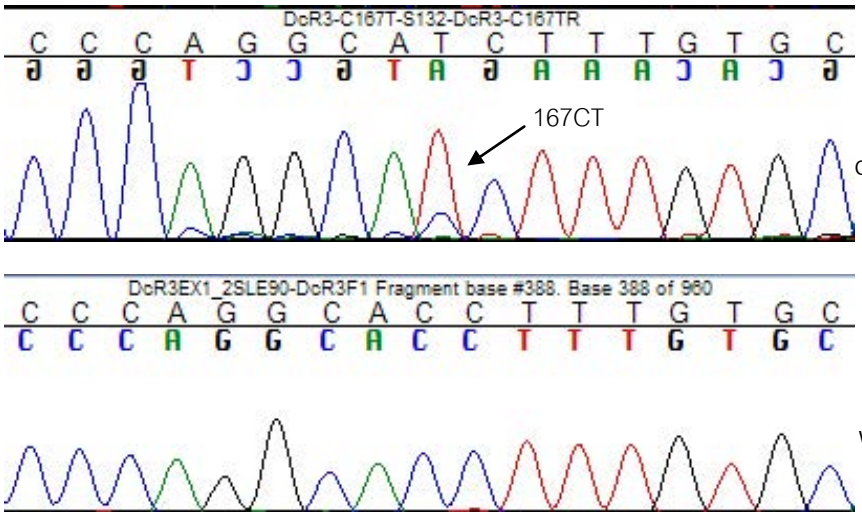

c.C167T *DcR3* (Adult SLE)

Wild type *DcR3*

B

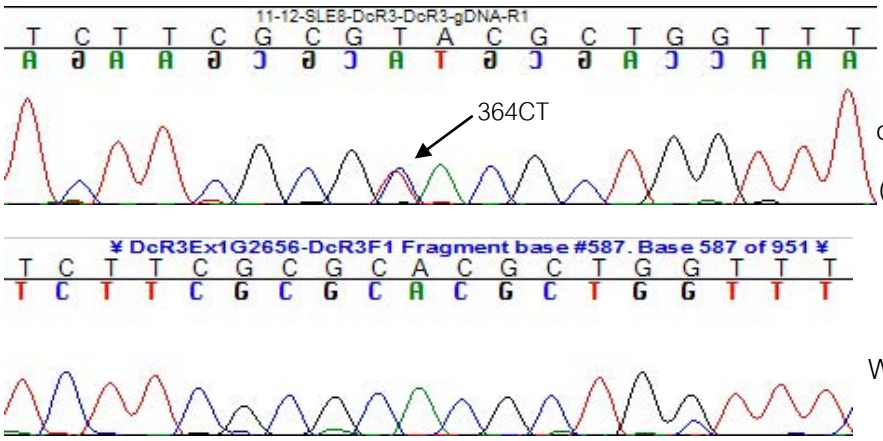

c.C364T *DcR3* (Juvenile SLE)

Wild type *DcR3*

C

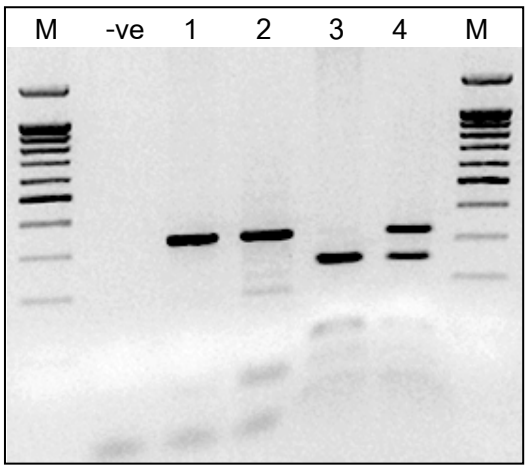

D

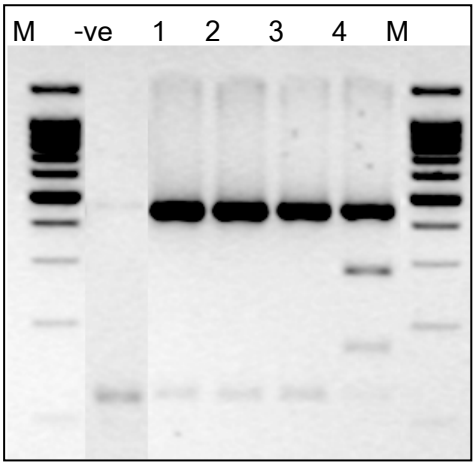

Figure 8. Chromatograms of mutations in the *DcR3* gene in adult and juvenile SLE patients and mutation confirmation by PCR-RFLP (A) Chromatograms of heterozygous c.C167T *DcR3* in adult SLE and wild type *DcR3* (B) Chromatograms of heterozygous c.C364T *DcR3* in juvenile SLE and wild type *DcR3* (C) Heterozygous c.C167T *DcR3* in adult SLE was confirmed by PCR-RFLP; -ve: negative control; lanes 1-2: PCR bands of an unaffected control (lane 1) and the adult SLE patient (lane 2); lanes 3-4: RFLP with *Ban*I (wild type cut) of PCR from an unaffected control (lane 3) and the adult SLE patient (lane 4) (D) Heterozygous c.C364T *DcR3* in juvenile SLE was confirmed by PCR-RFLP; -ve: negative control; lanes 1-2: PCR bands of an unaffected control (lane 1) and the juvenile SLE patient (lane 2); lanes 3-4; RFLP with *Rsa*I (mutant cut) of PCR from an unaffected control (lane 3) and the juvenile SLE patient (lane 4)

Clinical features of patients with *DcR3* mutations

The juvenile SLE patient had thrombocytopenic purpura when she was 8 years old. At the age of 16, she developed oral ulcer at the hard palate, malar rash, discoid rash, and lupus nephritis. She also had positive antinuclear-antibody and anti-double-stranded DNA.

The adult SLE patient was diagnosed with discoid rash erythematosus (DLE) when she was 25 years old. A year later, she had oral ulcer, malar rash, photosensitive skin, and lupus nephritis.

Mutant allele investigation in SLE parents and controls

We sequenced the *DcR3* gene to investigate mutant alleles in SLE parents. The C167T and C364T alleles were inherited from the mothers of SLE patients. Then we did PCR-RFLP to explore the mutant alleles in 500 unaffected controls. Interestingly, there was no C167T allele in 1,000 alleles of unaffected controls. In contrast, there was one allele in an affected control. Then, we did PCR and sequencing in the unaffected control to confirm that she had C364T allele.

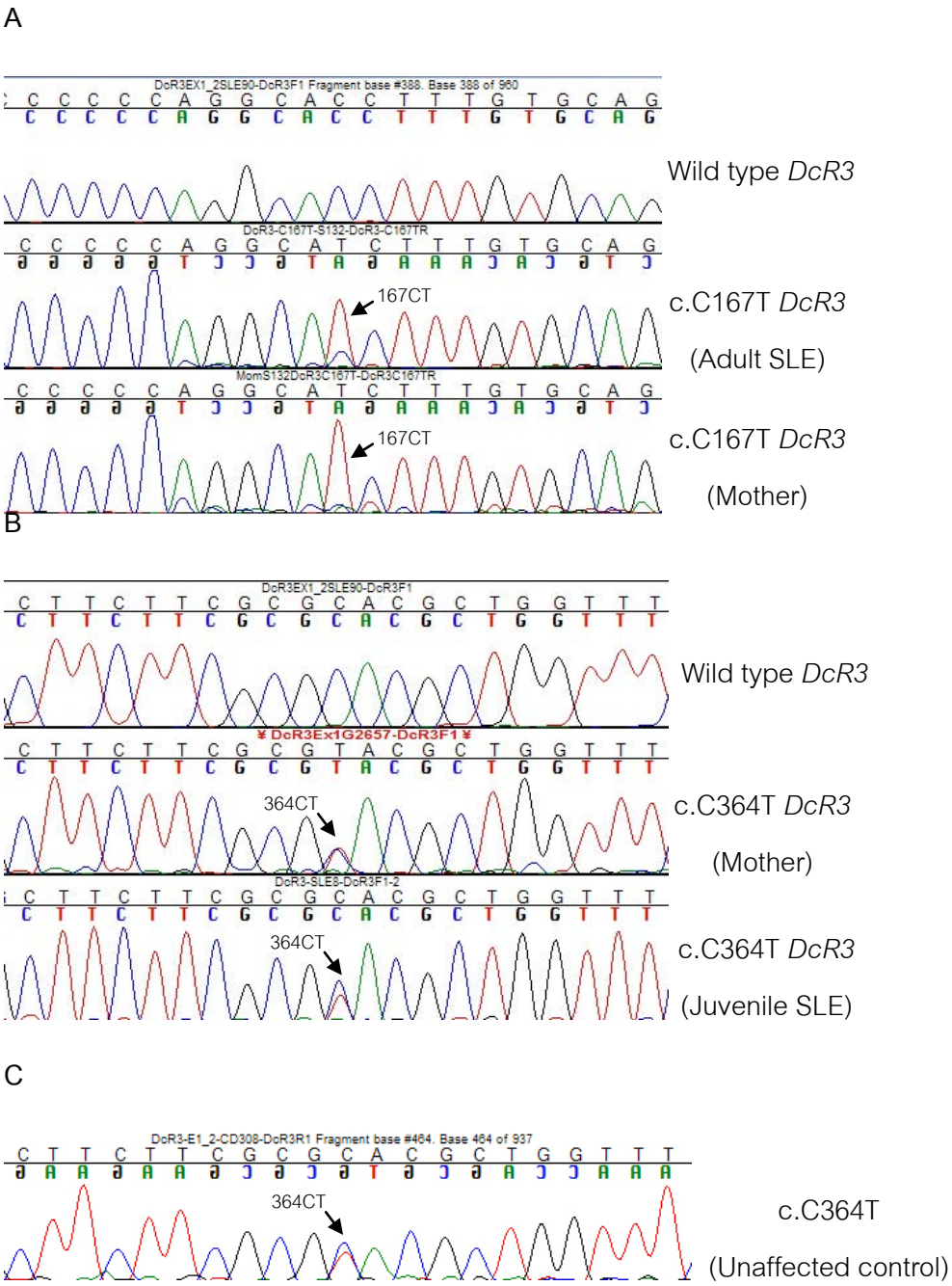

Figure 9. Chromatograms of mutations in the *DcR3* gene in both SLE mothers and one unaffected control (A) Chromatograms of heterozygous c.C167T *DcR3* in the adult SLE , her mother and wild type *DcR3* (B) Chromatograms of heterozygous c.C364T *DcR3* in juvenile SLE, her mother, and wild type *DcR3* (C) A chromatogram of c.C364T *DcR3* in the unaffected control

Type of mutation and mutation analysis

The c.C167T and c.C364T mutations in the *DcR3* gene resulted in isoleucine substitution in position 56 (T56I) and tyrosine substitution in position 122 (H122Y) respectively. For T56I, threonine is an uncharged polar amino acid with a hydroxyl group whereas isoleucine is a nonpolar neutral amino acid. For H122Y, histidine is a basic and positively charged amino acid whereas tyrosine is uncharged polar amino acid with a hydroxyl group.

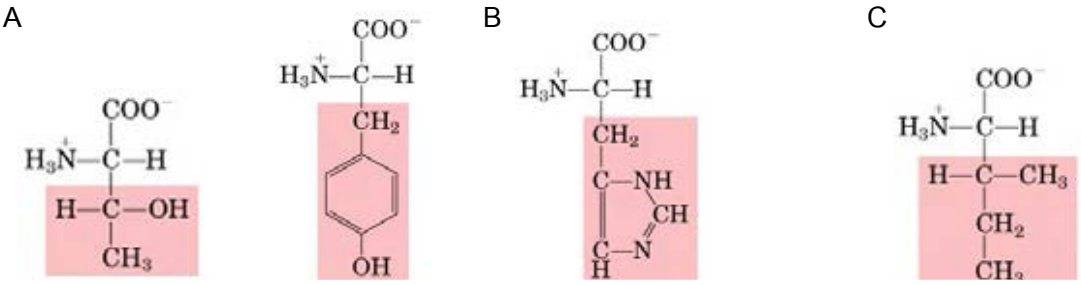

Figure 10. Amino acid classification of the wild type and mutant DcR3; (A) Uncharged polar amino acid with hydroxyl group; (B) Basic and positively charged amino acid; (C) Nonpolar neutral amino acid; Amino acid classification according to 4th Edition Human Molecular Genetics, Garland Science

DcR3 protein sequence analysis

To examine the evolutionary conservation of DcR3 protein, particularly in the positions of mutations found in the SLE patients, DcR3 protein sequences from nine 14 vertebrate species which were obtained from sequences available from Ensenbl database were aligned using ClustralX2 software. The threonine at position 56 of human DcR3 is conserved among all 14 vertebrate species. The histidine at position 122 of human DcR3 is conserved only 5 from 14 vertebrate species including human (*Homo sapiens)*, panda (*Ailuropoda melanoleuca)*, cow (*Bos taurus)*, elephant (*Loxodonta africana)*, and Tasmanian devil (*Sarcophilus harrisii)* which they are mammalian species.

A

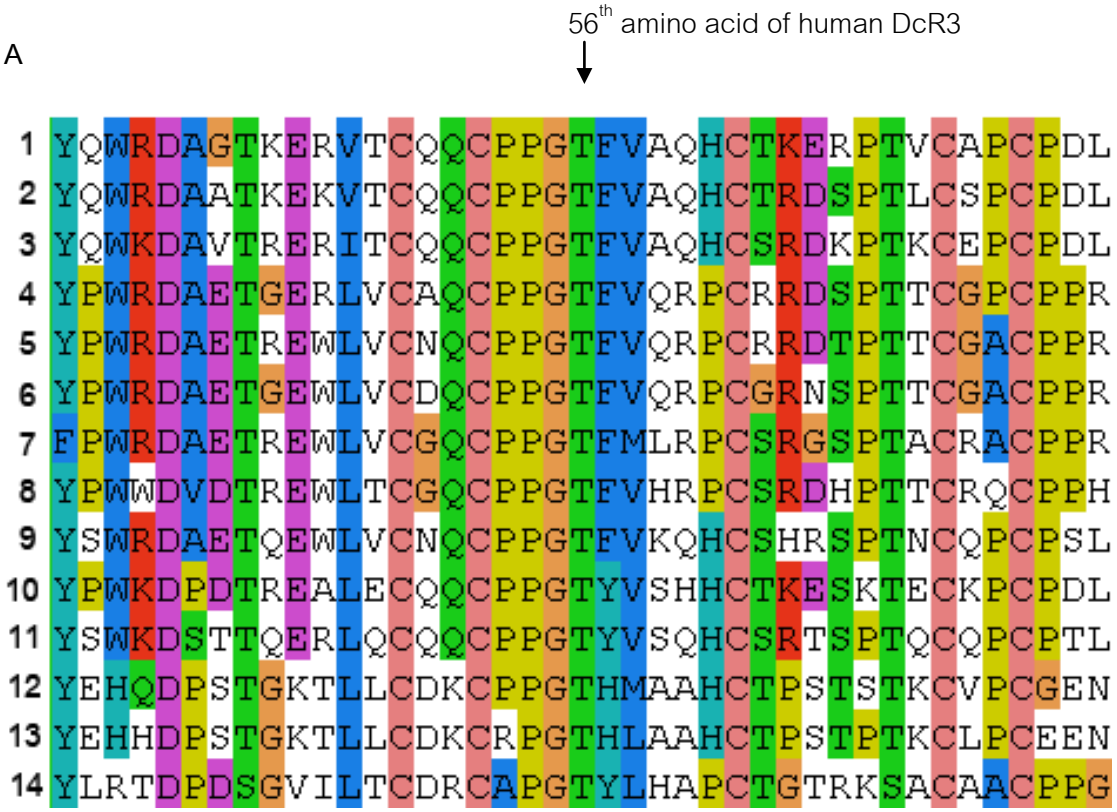
56th amino acid of human DcR3
1 YQWRDAGTKERVTCQQCPPGTFVAQHCTKERPTVCAPCPDL
2 YQWRDAATKEKVTCQQCPPGTFVAQHCTRDSPTLCSPCPDL
3 YQWKDAVTRERITCQQCPPGTFVAQHCSRDKPTKCEPCPDL
4 YPWRDAETGERLVCAQCPPGTFVQRPCRRDSPTTCGPCPPR
5 YPWRDAETREWLVCNQCPPGTFVQRPCRRDTPTTCGACPPR
6 YPWRDAETGEWLVCDQCPPGTFVQRPCGRNSPTTCGACPPR
7 FPWRDAETREWLVCGQCPPGTFMLRPCSRGSPTACRACPPR
8 YPWWDVDTREWLTCGQCPPGTFVHRPCSRDHPTTCRQCPPH
9 YSWRDAETQEWLVCNQCPPGTFVKQHCSHRSPTNCQPCPSL
10 YPWKDPDTREALECQQCPPGTYVSHHCTKESKTECKPCPDL
11 YSWKDSTTQERLQCQQCPPGTYVSQHCSRTSPTQCQPCPTL
12 YEHQDPSTGKTLLCDKCPPGTHMAAHCTPSTSTKCVPCGEN
13 YEHHDPSTGKTLLCDKCRPGTHLAAHCTPSTPTKCLPCEEN
14 YLRTDPDSGVILTCDRCAPGTYLHAPCTGTRKSACAACPPG

B

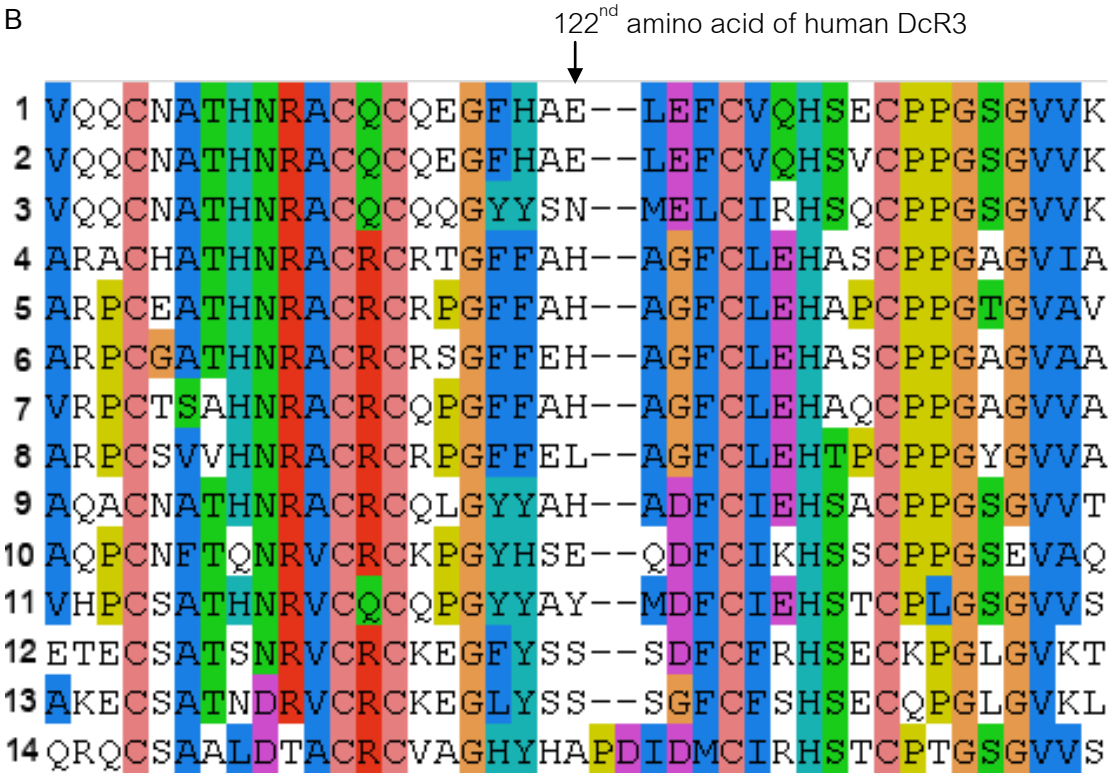
122nd amino acid of human DcR3
1 VQQCNATHNRACQCQEGFHAE--LEFCVQHSECPPGSGVVK
2 VQQCNATHNRACQCQEGFHAE--LEFCVQHSVCPPGSGVVK
3 VQQCNATHNRACQCQQGYYSN--MELCIRHSQCPPGSGVVK
4 ARACHATHNRACRCRTGFFAH--AGFCLEHASCPPGAGVIA
5 ARPCEATHNRACRCRPGFFAH--AGFCLEHAPCPPGTGVAV
6 ARPCGATHNRACRCRSGFFEH--AGFCLEHASCPPGAGVAA
7 VRPCTSAHNRACRCQPGFFAH--AGFCLEHAQCPPGAGVVA
8 ARPCSVVHNRACRCRPGFFEL--AGFCLEHTPCPPGYGVVA
9 AQACNATHNRACRCQLGYYAH--ADFCIEHSACPPGSGVVT
10 AQPCNFTQNRVCRCKPGYHSE--QDFCIKHSSCPPGSEVAQ
11 VHPCSATHNRVCQCQPGYYAY--MDFCIEHSTCPLGSGVVS
12 ETECSATSNRVCRCKEGFYSS--SDFCFRHSECKPGLGVKT
13 AKECSATNDRVCRCKEGLYSS--SGFCFSHSECQPGLGVKL
14 QRQCSAALDTACRCVAGHYHAPDIDMCIRHSTCPTGSGVVS

Figure 11. Alignment of DcR3 orthologues from 14 vertebrate species including 1: *Gallus gallus* (Chicken); 2: *Meleagris gallopavo* (Turkey); 3: *Taeniopygia guttata* (Zebra finch); 4: *Homo sapiens* (Human); 5: *Ailuropoda melanoleuca* (Panda); 6: *Bos taurus* (Cow); 7: *Loxodonta africana* (Elephant); 8: *Myotis lucifugus* (little brown bat); 9: *Sarcophilus harrisii* (Tasmanian devil); 10: *Anolis carolinensis* (Anole lizard); 11: *Ornithorhynchus anatinus*(Platypus); 12: *Takifugu rubripes* (Puffer fish); 13: *Tetraodon nigroviridis* (Green spotted puffer fish); 14: *Gadus morhua* (Alantic cod) (A) Alignment covering 56thamino acid (p.T56I, adult SLE) (B) Alignment covering 122ndamino acid (p.H122Y, juvenile SLE)

Prediction of impact of mutations on DcR3 protein

Two amino acid substitutions in the *DcR3* gene were predicted whether they might affect the protein function by PolyPhen and SIFT online software. The results are shown in table 4.

Table 4. Prediction of the impact of mutations on DcR3 protein

Mutation	Prediction	
	PolyPhen	SIFT
p.T56I (adult SLE)	Probably damaging	Deleterious
p.H122Y (juvenile SLE)	Possibly damaging	Tolerated

DcR3-Fc expression vector construction

The pRK5-*DcR3-Fc* vector was a gift from Genetech, USA. The vector was verified by RFLP and sequencing. All nucleotide sequence and *DcR3-Fc* insert size were correct. We did site-directed mutagenesis to introduce mutations including c.C167T (p.T56I, adult SLE) and c.C364T (p.H122Y, juvenile SLE) into the pRK5-*DcR3-Fc* vector. The mutagenized nucleotides including c.C167T and c.C364T were then verified by PCR-RFLP and sequencing (Figure 12).

A

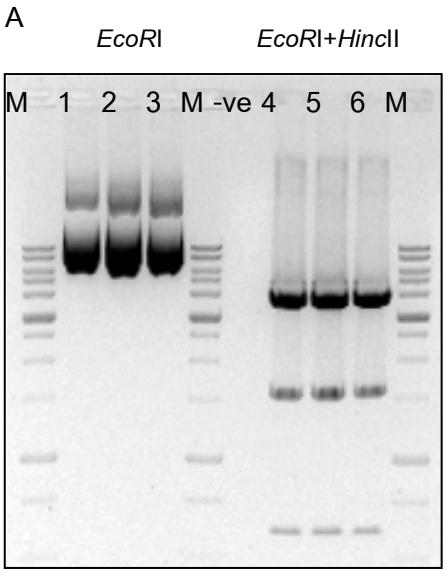

B

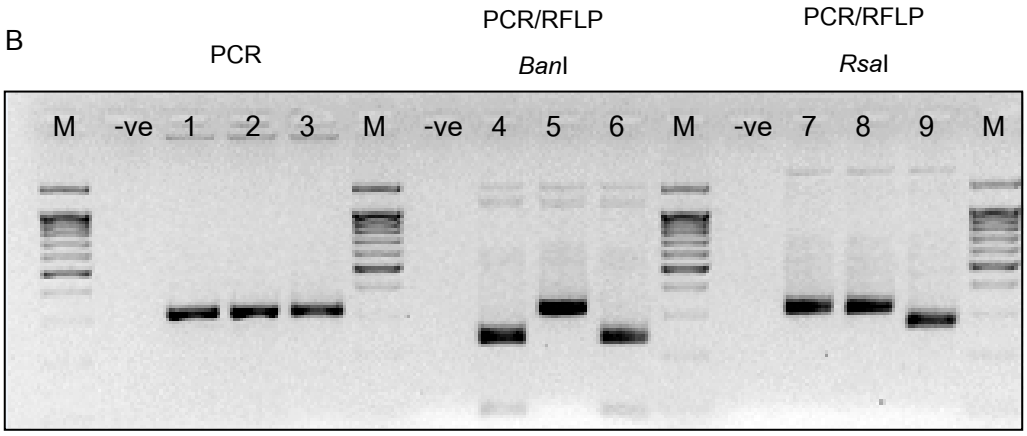

C

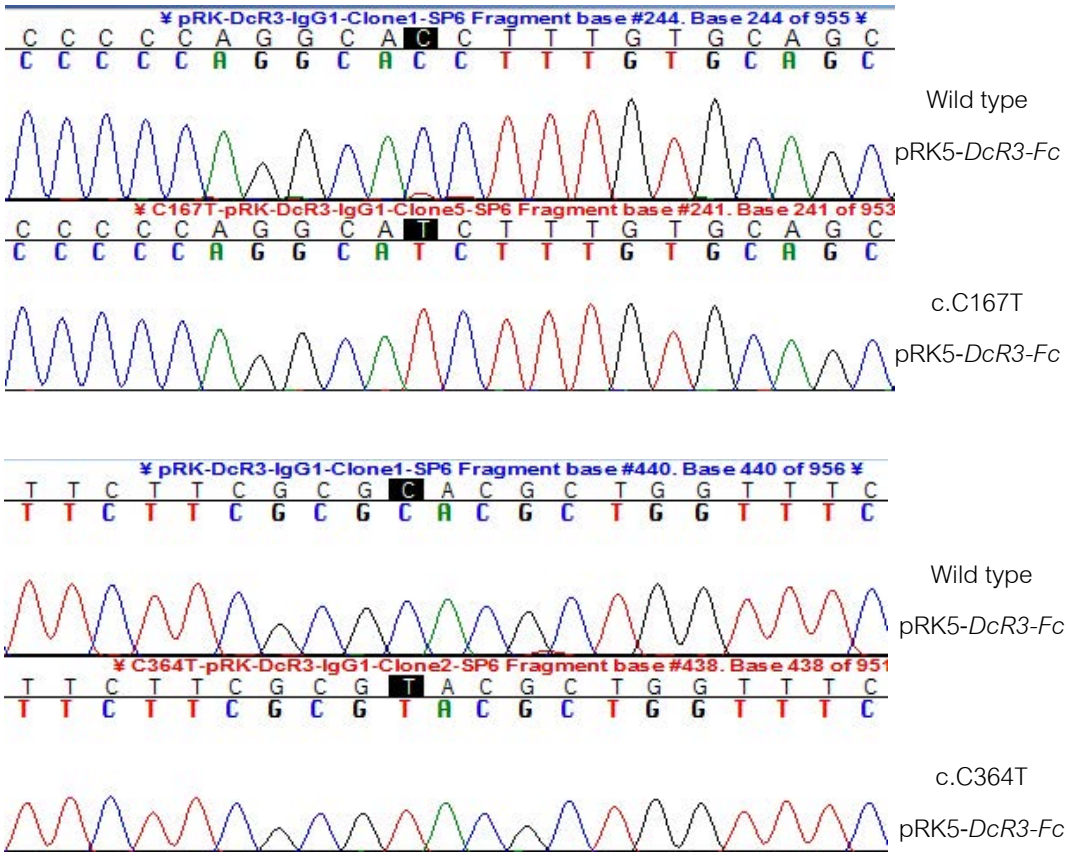

Figure 12. Site-directed mutagenesis in *DcR3-Fc* and vector verification; (A) RFLP of wild type, c.C167T, and c.C364T pRK5-*DcR3-Fc* vectors by *Eco*RI (lane1-3) and *Eco*RI+*Hinc*II (lane 4-6); M: 1 kb M11 DNA ladder (with bands at 10,000, 8,000, 6,000, 5,000, 4,000, 3,000, 2,500, 2,000, 1,500, 1,000, and 750 base pairs); lane 1,4: wild type pRK5-*DcR3-Fc*; lane 2,5: c.C167T pRK5-*DcR3-Fc*; lane 3,6: c.C364T pRK5-*DcR3-Fc*; RFLP by *Eco*RI showing linear size of pRK5-*DcR3-Fc* vector estimated 6,000 base pairs (the actual size of vector is 6,233 base pairs); RFLP by *Eco*RI and *Hinc*II showing the pRK5 backbone estimated 4,000 and below 750 base pairs (the actual size of pRK5 back bone is 4,626 base pairs and *Hinc*II digested to two sites in pRK5 backbone) and *DcR3-Fc* insert estimated 1,500 base pairs (the actual size of insert *DcR3-Fc* is 1,607 base pairs) (B) PCR-RFLP of wild type and mutant pRK5-*DcR3-Fc* vectors by specific primers (lane 1-9) and digested with *Ban*I (lane 4-6)/*Rsa*I (lane 7-9); M: 100 bp M23 DNA ladder (with bands at 1,500, 1,000, 901, 801, 701, 601, 500, 401, 301, and 201

base pairs) lane 1,4,7: wild type pRK5-*DcR3-Fc*; lane 2,5,8: c.C167T pRK5-*DcR3-Fc*; lane 3,6,9: c.C364T pRK5-*DcR3-Fc*; PCR product size is 316 base pairs. The c.C167T was uncleaved by *Ban*I and c.C364T was cleaved by *Rsa*I. (C) Chromatograms showing c.C167T and c.C364T were introduced into pRK5-*DcR3-Fc* vector.

The wild type and both mutant, C167T and C364T, *DcR3-Fc* were sub-cloned into the pIRES2-*EGFP* expression vector. The pIRES2-*EGFP* vector was digested with *EcoR*I (sticky end at 5') and *Sma*I (blunt end at 3'). Wild type, c.C167T and c.C364T DcR3-*Fc* were digested from pRK5 vector by *EcoR*I (sticky end at 5') and *Hinc*II (blunt end at 3'). Then the *EcoR*I/*Hinc*II digested *DcR3-Fc* fragments were ligated to the *EcoR*I/*Sma*I digested pIRES2-*EGFP* vector and transformed into *E. coli DH5*α. All vectors were verified by RFLP, PCR-RFLP, and sequencing (Figure 13).

A

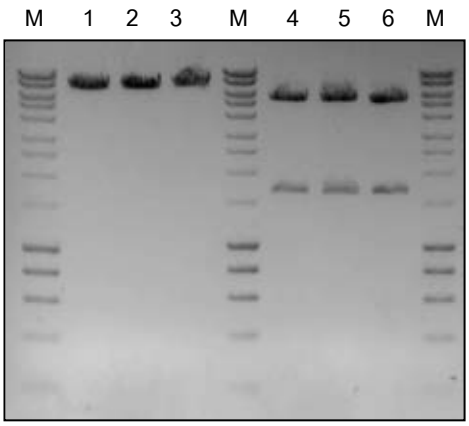

B

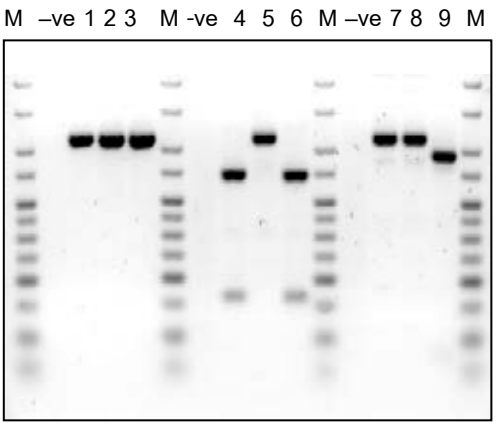

C

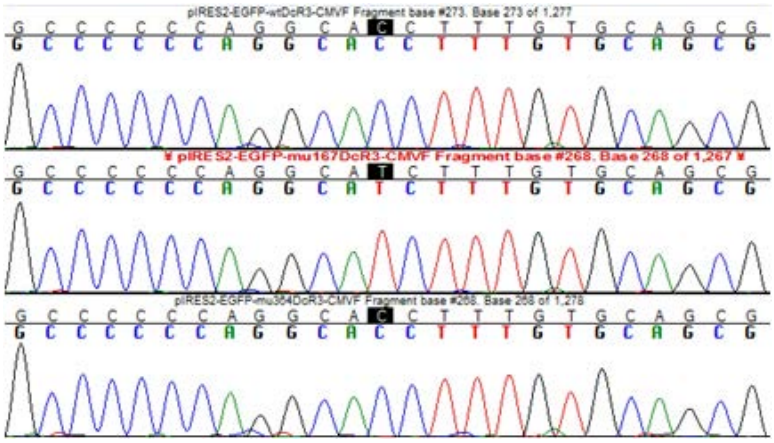

Wild type

pIRES2-*EGFP-DcR3-Fc*

c.C167T

pIRES2-*EGFP-DcR3-Fc*

c.C364T

pIRES2-*EGFP-DcR3-Fc*

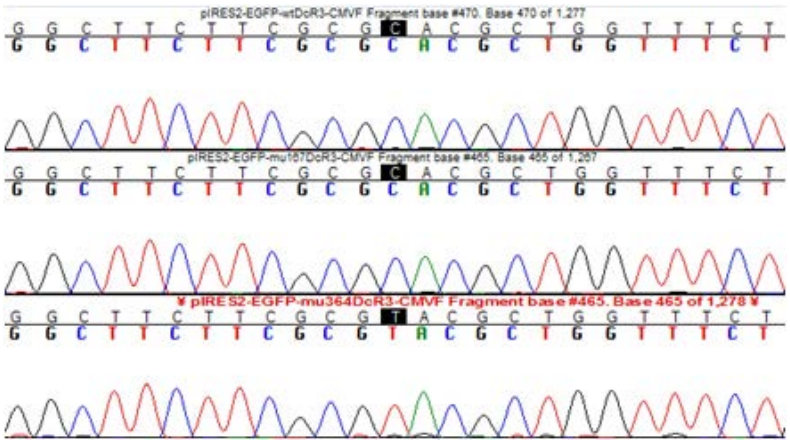

Wild type

pIRES2-*EGFP-DcR3-Fc*

c.C167T

pIRES2-*EGFP-DcR3-Fc*

c.C364T

pIRES2-*EGFP-DcR3-Fc*

Figure 13. Sub-cloning of the wild type, c.C167T, and c.C364T *DcR3-Fc* to the pIRES2-*EGFP* expression vector; (A) RFLP of pIRES2-*EGFP*-*DcR3-Fc* vector by *Eco*RI (lanes 1-3) and *Eco*RI/*BamH*I (lanes 4-6); M: HyperLadder™I (with bands 10,000, 8,000, 6,000, 5,000, 4,000, 3,000, 2,500, 2,000, 1,500, 1,000, 800, 600 and 400 base pairs); lanes 1,4: wild type pIRES2-*EGFP*-*DcR3-Fc* lanes 2,5: c.C167T pIRES2-*EGFP*-*DcR3-Fc* lanes 3,6: c.C364T pIRES2-*EGFP*-*DcR3-Fc*; RFLP by *Eco*RI showing linear size of pIRES2-*EGFP*-*DcR3-Fc* vector between 8,000 and6,000 base pairs (the actual size of vector is 6.9 kb); RFLP by *Eco*RI and *BamH*I showing the pIRES2-*EGFP* backbone between 6,000 and 5,000 base pairs (the actual size of pIRES2-*EGFP* back bones is 5.3 kb) and *DcR3-Fc* insert between 2,000 and 1,500 base pairs (the actual size of insert *DcR3-Fc* is 1.6 kb) (B) PCR-RFLP of wild type, c.C167T, and c.C364T pIRES2-*EGFP*-*DcR3-F*c vectors (lanes 1-9) and PCR digested with *Ban*I (lanes 4-6)/*Rsa*I (lane 7-9); M: HyperLadder™V (with bands at 500, 400, 300, 250, 200, 175, 150, 125, 100, 75, 50, and 25 base pairs) lanes 1,4,7: wild type pIRES2-*EGFP*-*DcR3-Fc*; lanes 2,5,8: c.C167T pIRES2-*EGFP*-*DcR3-Fc*; lanes 3,6,9: c.C364T pIRES2-*EGFP*-*DcR3-Fc*; PCR product size is 316 base pairs. The c.C167T was uncleaved by *Ban*I and c.C364T was cleaved by *Rsa*I. (C) Chromatograms showing the nucleotide sequencing of the wild type, c.C167T, and c.C364T pIRES2-*EGFP*-*DcR3-Fc* vector

Wild type, p.T56I and p.H122Y DcR3-Fc protein production

The expression vectors containing the wild type, c.C167T, and c.C364T *DcR3-Fc* were transiently transfected into COS1 or COS-7 cell line. Lipofectamine™2000 reagent was used to deliver vectors into the cells. The optimal DNA and Lipofectamine™2000 ration is 1:2.5. Transfection efficiency was determined using flow cytometry and fluorescent microscopy by GFP expressed cells (Figures 14A and B). DcR3-Fc expression was examined by Western Blot with antibody specific to human DcR3. The secretion of wild type, p.T56I and p.H122Y DcR3-Fc from cells to culture supernatants was checked by Western Blot (Figures 14C and D). Then culture supernatants were harvested and dialyzed against 20 mM sodium phosphate buffer. The dialyzed supernatants were applied to HiTrap™ Protein G HP Column to purify DcR3-Fc. The purity of protein was checked by Coomassie blue staining and the purified proteins were examined again by Western blot (Figures 14E, F, G and H). Then they were used for functional studies.

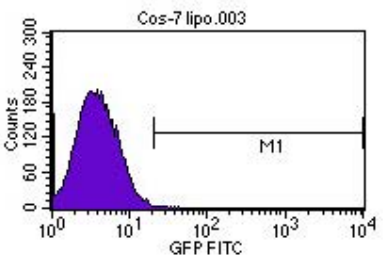

Sample ID: Cos-7 lipo
Gated Events: 28340
Total Events: 30000

Left, Right	% Gated	% Total	Mean
1, 9910	100.00	94.47	4.32
21, 9910	0.08	0.08	24.97

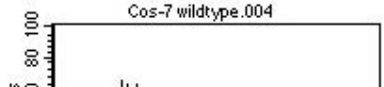

Sample ID: Cos-7 wildtype
Gated Events: 24389
Total Events: 30000

A

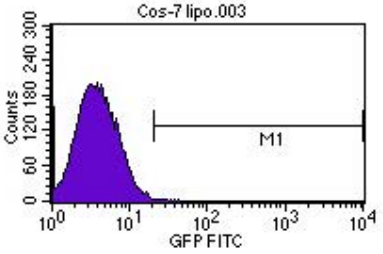

Sample ID: Cos-7 lipo
Gated Events: 28340
Total Events: 30000

Left, Right	% Gated	% Total	Mean
1, 9910	100.00	94.47	4.32
21, 9910	0.08	0.08	24.97

Lipofectamine™2000

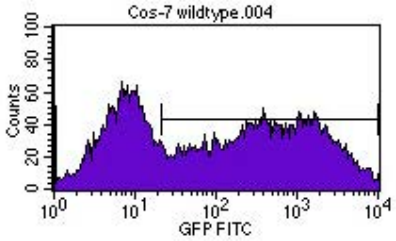

Sample ID: Cos-7 wildtype
Gated Events: 24389
Total Events: 30000

Left, Right	% Gated	% Total	Mean
1, 9910	100.00	81.30	649.96
21, 9910	64.07	52.09	1009.89

Lipofectamine™2000 +

Wild type pIRES2-*EFGP-DcR3-Fc*

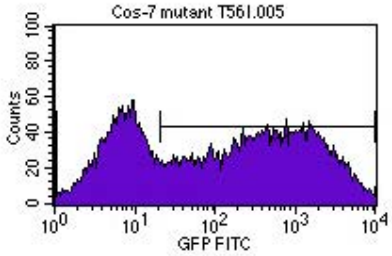

Sample ID: Cos-7 mutant T56I
Gated Events: 23726
Total Events: 30000

Left, Right	% Gated	% Total	Mean
1, 9910	100.00	79.09	670.33
21, 9910	66.13	52.30	1009.66

Lipofectamine™2000 +

c.C167T pIRES2-*EFGP-DcR3-Fc*

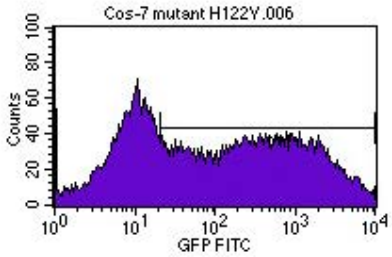

Sample ID: Cos-7 mutant H122Y
Gated Events: 23667
Total Events: 30000

Left, Right	% Gated	% Total	Mean
1, 9910	100.00	78.89	609.34
21, 9910	64.91	51.21	933.77

Lipofectamine™2000 +

c.C364T pIRES2-*EFGP-DcR3-Fc*

B

Lipofectamine™2000

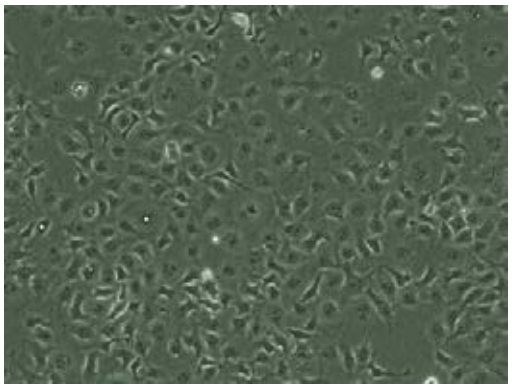

Lipofectamine™2000 +

wild type pIRES2-*EFGP-DcR3-Fc*

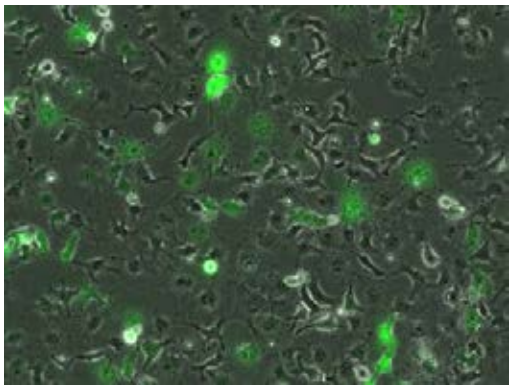

Lipofectamine™2000 +

c.C167T pIRES2-*EFGP-DcR3-Fc*

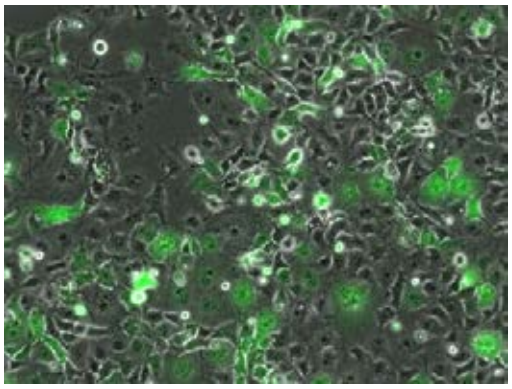

Lipofectamine™2000 +

c.C364T pIRES2-*EGFP-DcR3-Fc*

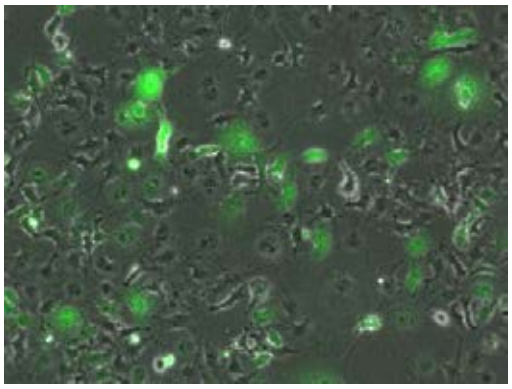

C

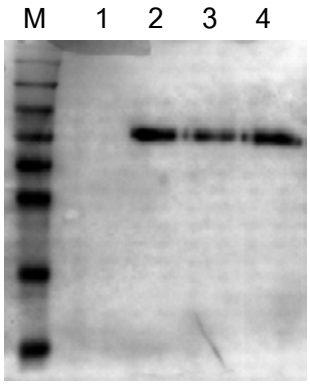

D

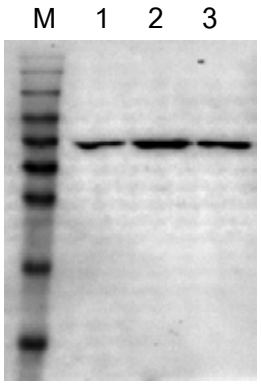

E

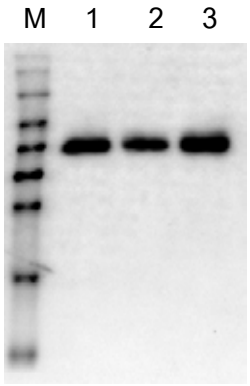

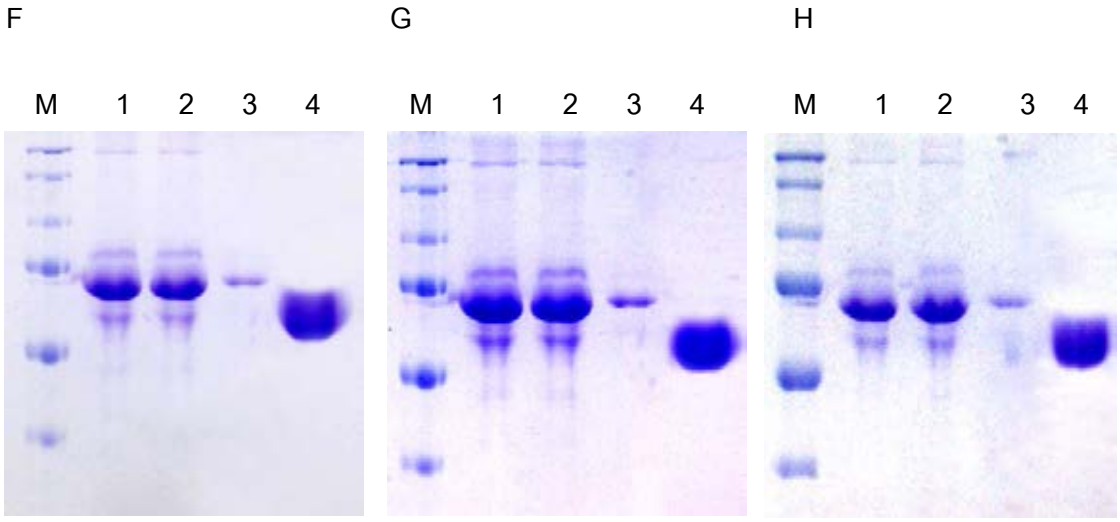

Figure 14. Wild type, p.T56I, and p.H122Y DcR3-Fc production (A-B) GFP expression in transfected COS7 (48 hours after transfection) visualized by (A) Flow cytometry and (B) fluorescent microscope; (C-E) Western Blot checking wild type, p.T56I and p.H122Y DcR3-Fc expression from COS7 or purified proteins (C) 24 hours after transfection; M: Chromatein Prestained Protein Ladder, Vivantis (with size: 175, 130, 95, 70, 62, 51 , 42, 29, and 22 kDa); lane 1: Lipofectamine™2000 only (negative control); lane 2: wild type pIRES2-*EGFP-DcR3-Fc* transfected COS7; lane 3: c.C167T pIRES2-*EGFP-DcR3-Fc* transfected COS7; lane 4: c.C364T pIRES2-*EGFP-DcR3-Fc* transfected COS7 (D) 48 hours after transfection; lane 1: wild type pIRES2-*EGFP-DcR3-Fc* transfected COS7; lane 2: c.C167T pIRES2-*EGFP-DcR3-Fc* transfected COS7; lane 3: c.C364T pIRES2-*EGFP-DcR3-Fc* transfected COS7 (E) Purified wild type, p.T56I and p.H122 DcR3-Fc from HiTrap™ Protein G HP column; lane 1: wild type *DcR3-Fc*; lane 2: p.T56I *DcR3-Fc*; lane 3: p.H122Y *DcR3-Fc* (F-G) Purity check of purified proteins by Coomassie blue staining; M: All Blue Stain Protein Ladder, Bio-Rad (with size: 250, 150, 100, 75, 50, and 37 kDa); lane 1: Supernatant; lane 2: Flowthrough; lane 3: Wash; lane 4: Purified (F) wild type DcR3-Fc (G) p.T56I DcR3-Fc and (H) p.H122Y DcR3-Fc

Protein binding affinity test by Surface Plasmon Resonance (SPR)

SPR technique was used to determine the affinity between the wild type and both mutants including p.T56I and p.H122Y versus immobilized FasL-FLAG. SPR kinetic analysis at equilibrium phase showed that the wild type and both mutants to FasL-FLAG at Kd of 128±1.1, 52.8±0.3, and 176±2.5 nM, respectively. The affinity of p.T56I DcR3-Fc to FasL-FLAG is about 2.4 fold greater than the wild type DcR3-Fc to FasL-FLAG, whereas the affinity of the p.H122Y DcR3-Fc to FasL-FLAG is about 0.7 fold lower than the wild type DcR3-Fc to FasL-FLAG (Figure 15).

A

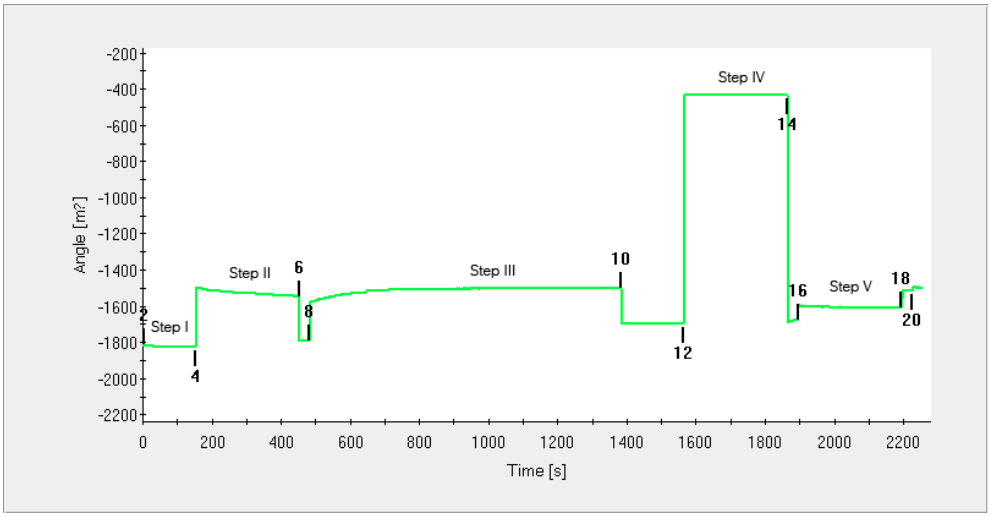

B

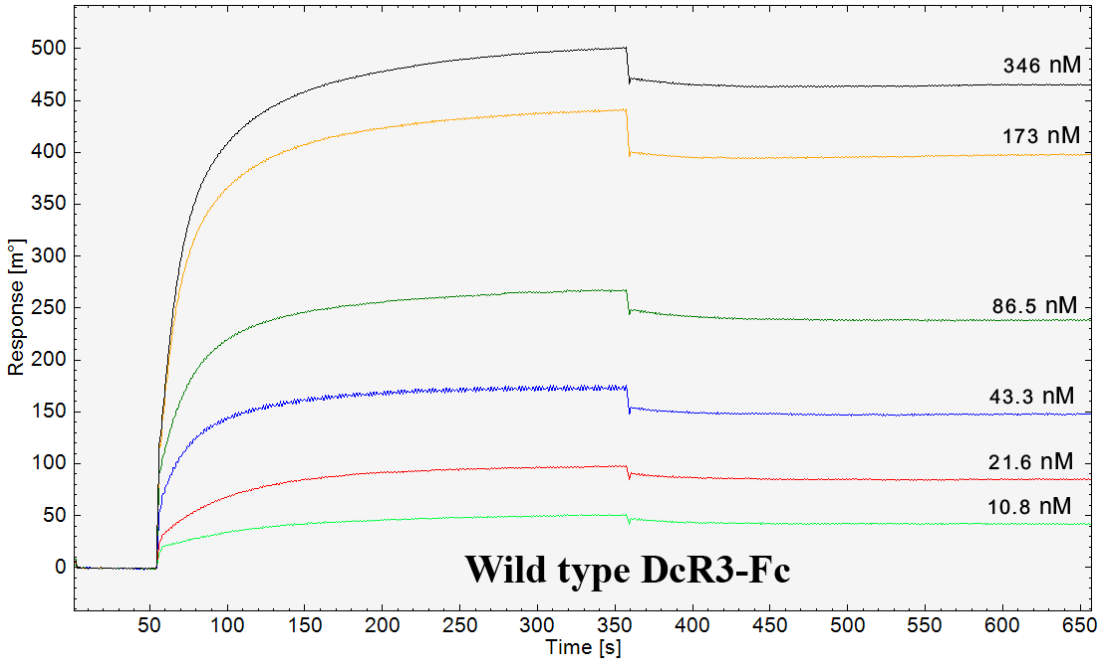
346 nM
173 nM
86.5 nM
43.3 nM
21.6 nM
10.8 nM
Wild type DcR3-Fc
Response [m°]
Time [s]

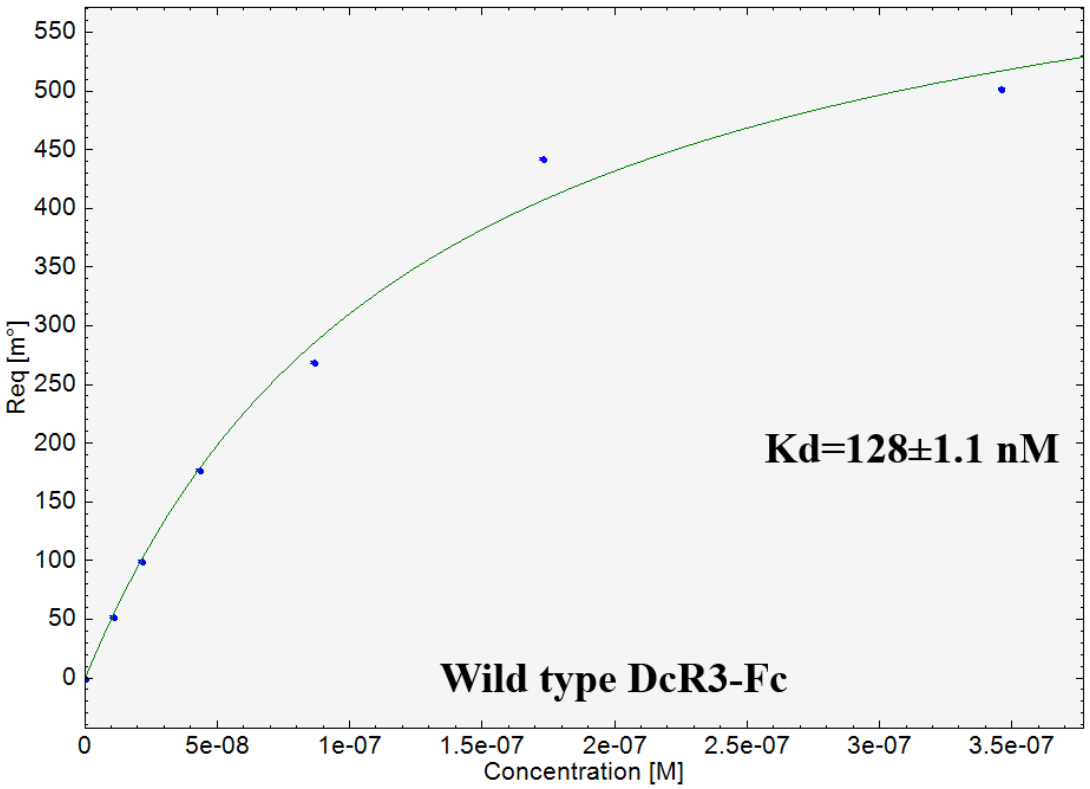
Kd=128±1.1 nM
Wild type DcR3-Fc
Req [m°]
Concentration [M]

C

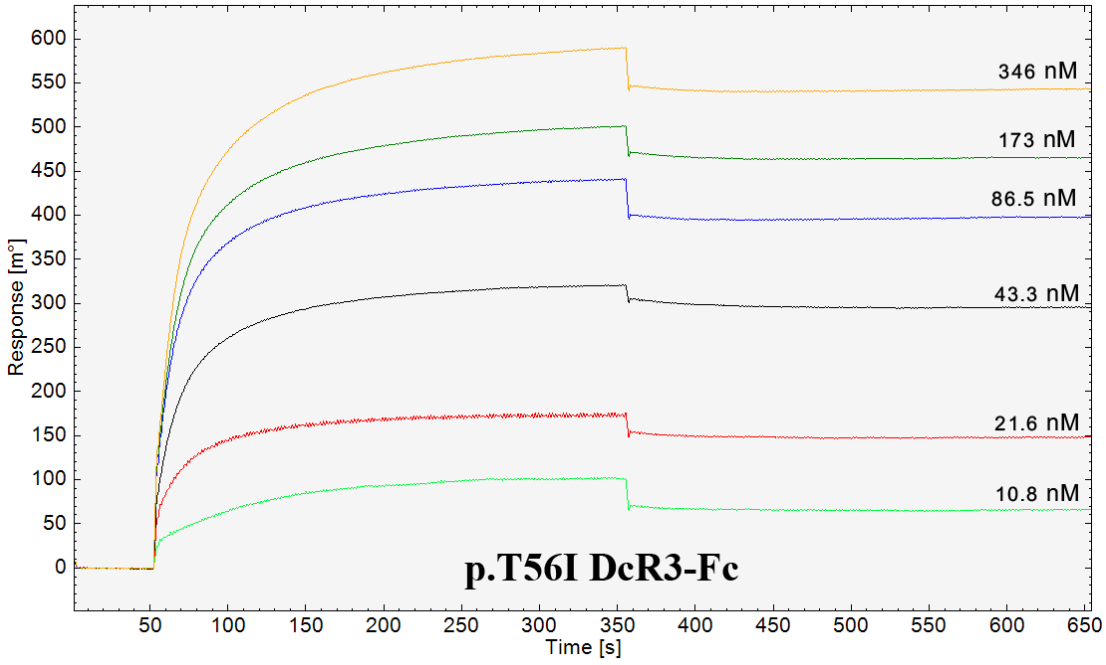
346 nM
173 nM
86.5 nM
43.3 nM
21.6 nM
10.8 nM
p.T56I DcR3-Fc
Response [m°]
Time [s]

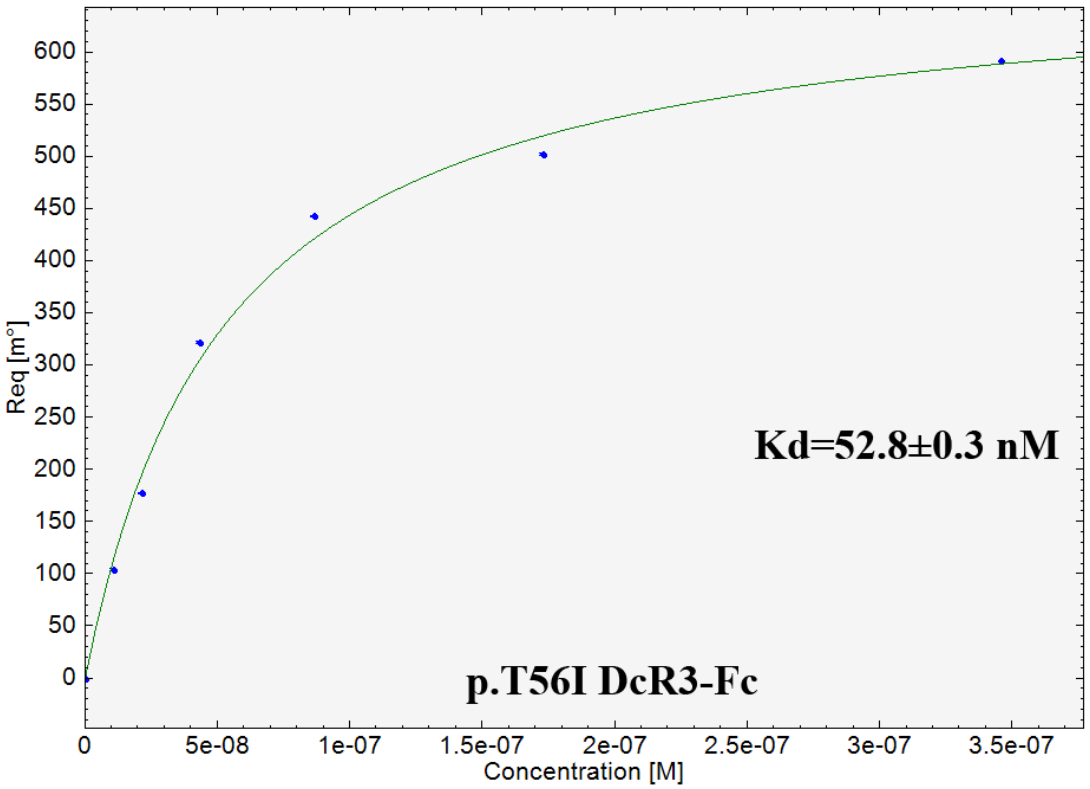
Kd=52.8±0.3 nM
p.T56I DcR3-Fc
Req [m°]
Concentration [M]

D

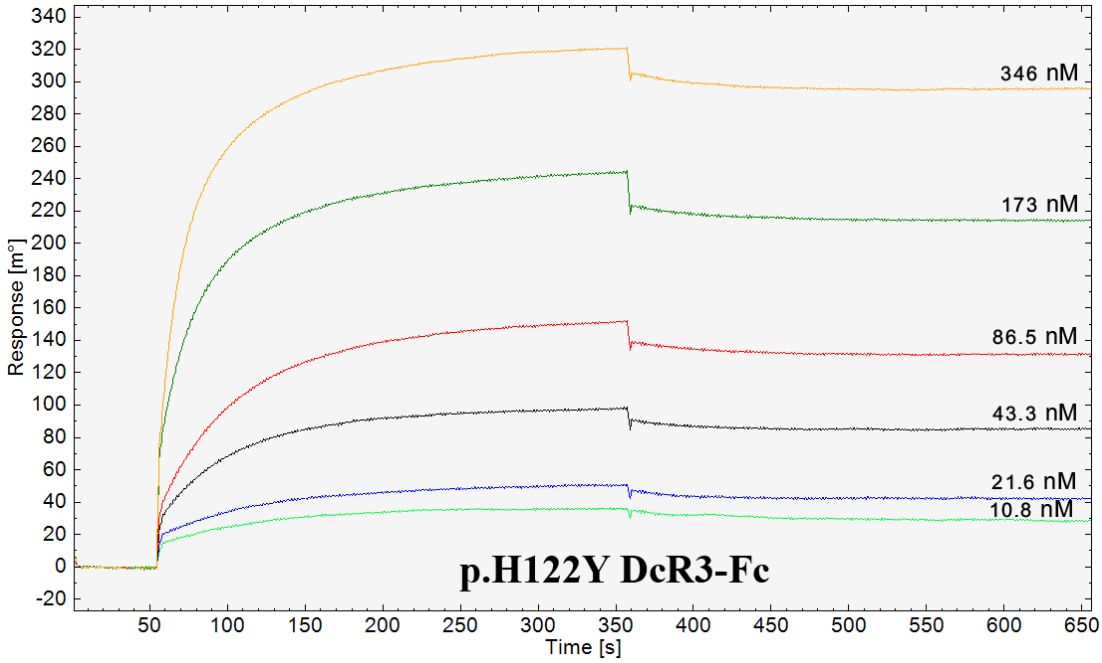
346 nM
173 nM
86.5 nM
43.3 nM
21.6 nM
10.8 nM
p.H122Y DcR3-Fc
Response [m°]
Time [s]

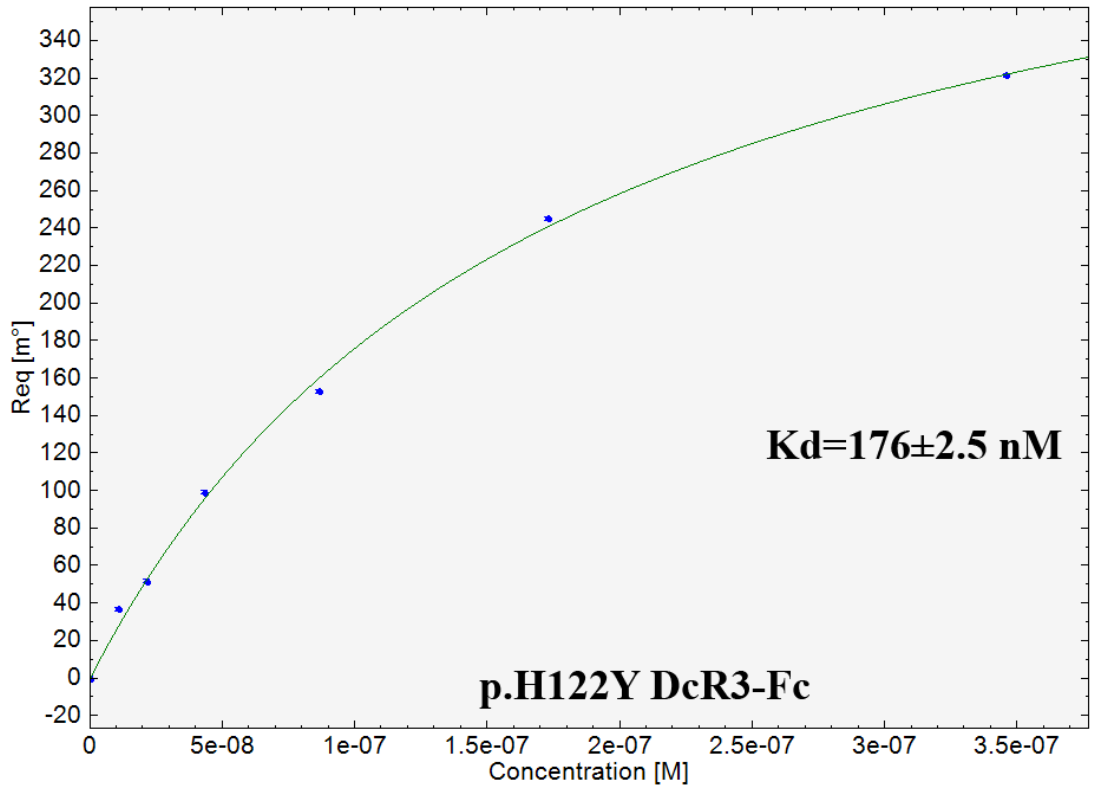
Kd=176±2.5 nM
p.H122Y DcR3-Fc
Req [m°]
Concentration [M]

Figure 15. Affinity test by SPR; (A) Step in immobilization of FasL-FLAG onto 50% surface grafted poly(acrylic acid) sensor chip by amine coupling reaction; Step I: Equilibration with 10 mM sodium acetate buffer pH4.5 for 150 seconds Step II: Activation with 0.1 M EDC and 0.1 M NHS for 5 minutes; Step III: Immobilization of 10 µg/ml FasL-FLAG in PBS for 15 minutes; Step IV: Blocking with 1.0 M Ethanolamine pH 8.5 for 5 minutes; Step V: Regeneration with 50 mM NaOH for 5 minutes; All SPR experiments, the level of immobilization was between 119 – 138.3 millidegrees corresponding to 99.2 – 115.3 ng protein/cm^2; (B-D) Overlaid sensograms of various concentrations of wild type, p.T56I, and p.H122Y DcR3-Fc binding to immobilized FasL-FLAG and equilibrium response value plotted against wild type, p.T56I, and p.H122Y DcR3-Fc concentrations assuming the monophasic association model; The equilibrium binding constant (Kd) was calculated from $Y = \frac{B_{max}X}{(K_d + X)}$, where B_{max} is the maximum specific binding.

Jurkat cells apoptosis assay

DcR3 plays a role in inhibiting FasL-induced apoptosis in Jurkat cells [55]. Therefore, we investigated the function of both mutants in FasL-induced Jurkat cell apoptosis. Firstly, we tested whether optimal concentrations of FasL to induce Jurkat cell apoptosis according to the manufacture's protocol. We found that the optimal concentration that gave the highest Jurkat cell apoptosis was 7.27 ng/ml FasL-FLAG cross linked with 0.25 µg/ml anti-FLAG. For this optimal condition, FasL-induced Jurkat cell had a significant increase in apoptosis ($p < 0.001$) (Figure 16A). Then we investigated whether the wild type DcR3-Fc inhibited FasL-induced Jurkat cell apoptosis. The wild type DcR3-Fc at concentration of 1 µg/ml significantly inhibited FasL-induced Jurkat cell apoptosis ($p<0.001$) (Figure 16B). Due to the Fc tag in DcR3-Fc, we also treated Jurkat cells with only Fc as a control of the experiment. We found that the Fc tag didn't have an effect on FasL-induced apoptosis in Jurkat cells (Figure 16B). To compare the ability of the wild type and both mutants including p.T56I and p.H122Y DcR3-Fc to suppress FasL-induced Jurkat cell apoptosis, we treated Jurkat cells with various concentrations of the wild type and both mutants (1000, 500, 250, 125, 50, and 1 ng/ml). There was no significantly different apoptosis between the wild type and both mutants at any concentration (Figure 16C).

A

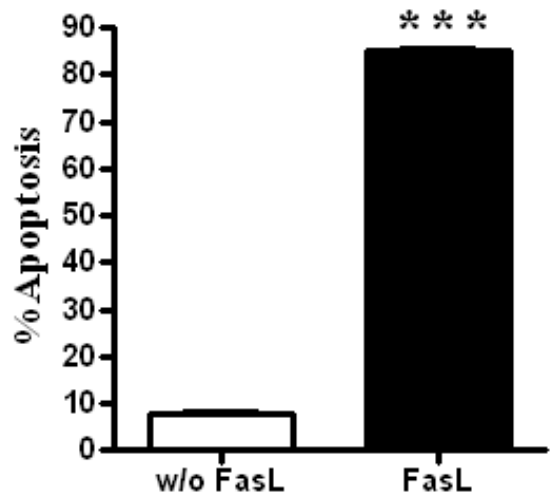
% Apoptosis
90
80
70
60
50
40
30
20
10
0
* * *
w/o FasL
FasL

B

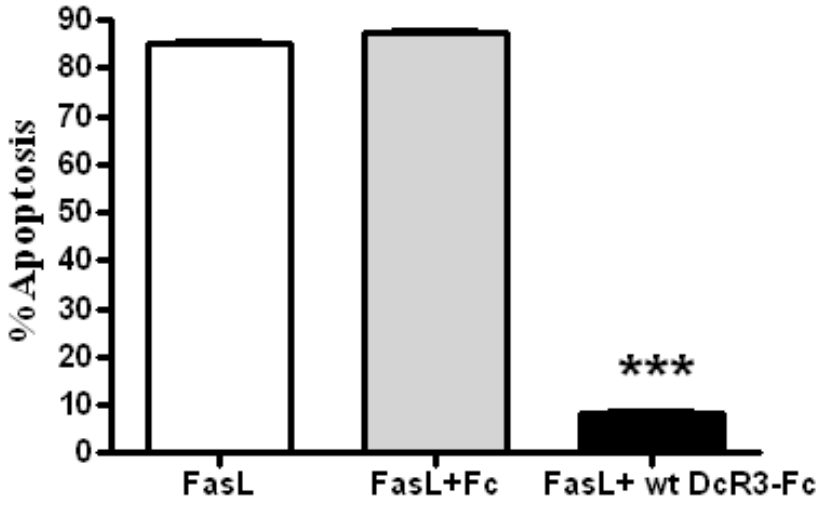
% Apoptosis
90
80
70
60
50
40
30
20
10
0
***
FasL
FasL+Fc
FasL+ wt DcR3-Fc

C

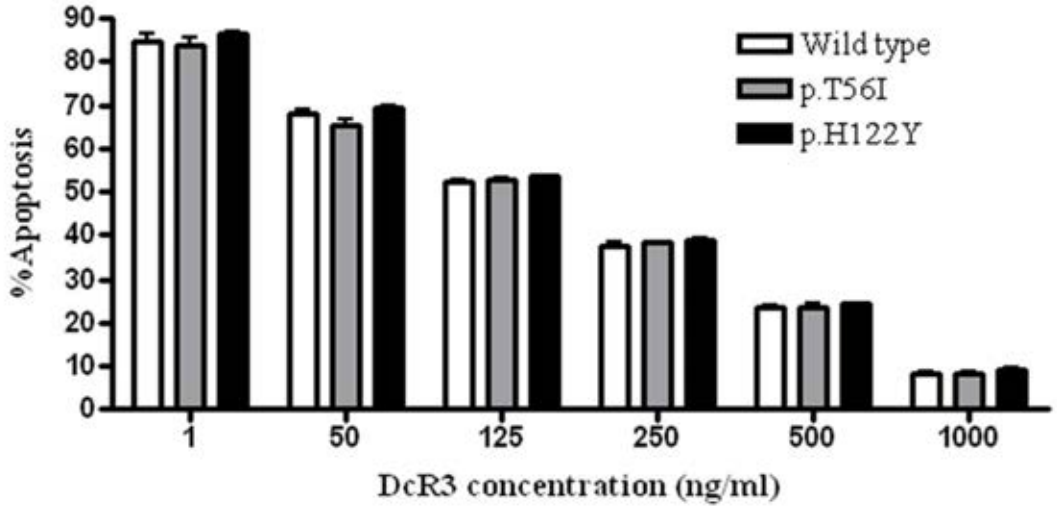

Figure 16. Jurkat cell apoptosis assay (A) FasL-induced Jurkat cell apoptosis; Jurkat cells were cultured for 16 hours in the presence or absence of 7.27 ng/ml FasL-FLAG cross linked with 0.25 μg/ml anti-FLAG. (B) Inhibition of FasL-induced Jurkat cell apoptosis by wild type DcR3-Fc; Jurkat cells were incubated with 7.27 ng/ml FasL-FLAG cross linked with 0.25 μg/ml anti-FLAG in the presence or absence of Fc (control) and wild type DcR3-Fc. (C) Inhibition of FasL-induced Jurkat cell apoptosis by wild type comparing to both mutants; Jurkat cells were incubated with 7.27 ng/ml FasL-FLAG cross linked with 0.25 μg/ml anti-FLAG in the presence or absence of various concentrations (indicated on the graph) of wild type and both mutants. Graphs represent mean ± standard deviation (SD) from triplicate experiment performing three different times. Statistical analyses were evaluated by Student *t*-test and the *p*-value less than 0.05 was considered as statistically significant (*$p<0.05$; **$p<0.01$; ***$p<0.001$).

Activation induced cell death (AICD) in lymphocytes

In addition to the ability of DcR3 in inhibition of FasL-induced apoptosis in Jurkat cells, DcR3 also plays a role in activation induced cell death (AICD) in peripheral blood T cells [19, 55]. Therefore, we investigated the function of both mutants, in lymphocytes AICD. Lymphocytes were isolated from peripheral blood and stimulated with phytohaemagglutinin (PHA) for 24 hours and then cultured in the presence of interleukin-2 (IL-2) for 5 days. The activated lymphocytes were then re-stimulated with plate-bound anti-CD3 in the presence or absence of the wild type and both mutants. The lymphocytes activated by anti-CD3 had a significant increase in AICD comparing to non-activated lymphocytes ($p < 0.01$) (Figure 17A). The wild type and both mutants with 20 μg/ml concentration significantly reduced AICD in lymphocytes ($p<0.01$) and 10 μg/ml Fc control didn't significantly reduce AICD in lymphocytes. However, there was no significant difference in reduced apoptosis between the wild type and both mutants (Figure 17A). The activated lymphocytes were then treated with other concentrations of the wild type and both mutants (10, 5, 1 μg/ml). There was no significant difference in reduced AICD between the wild type and both mutants at any concentration (Figure 17B).

A

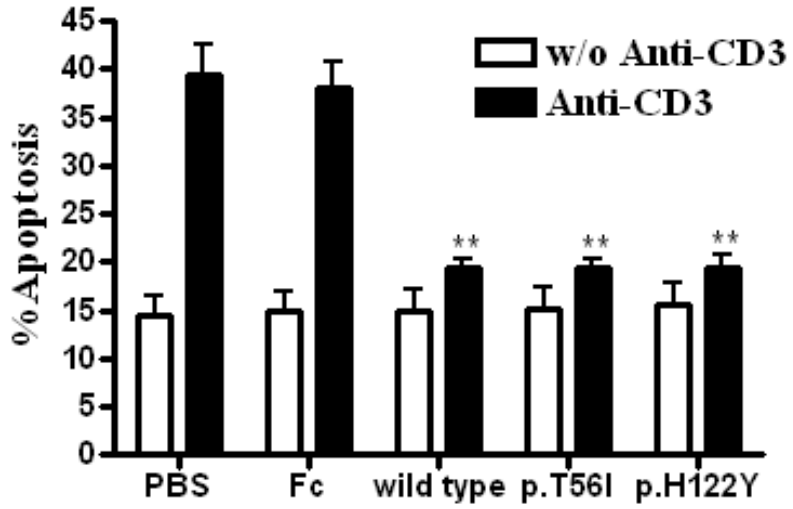

B

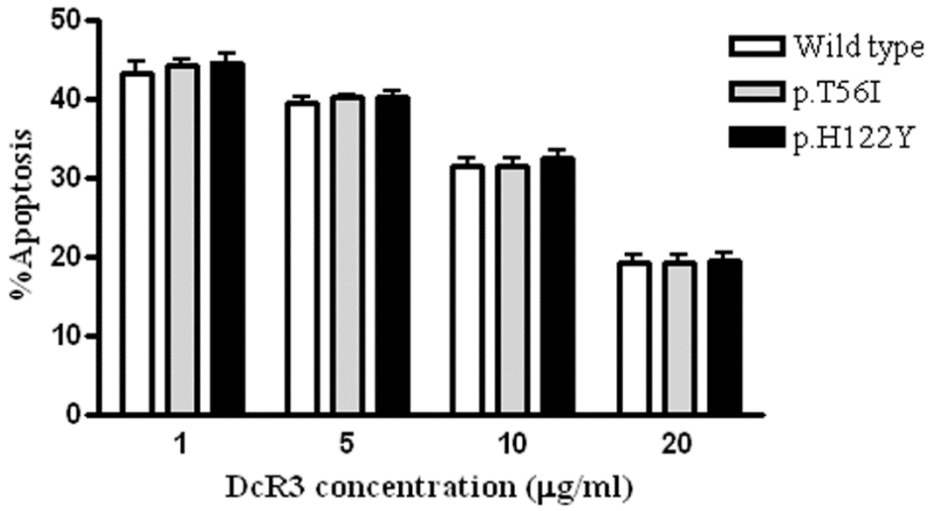

Figure 17. Activation induced cell death (AICD) in lymphocytes (A) Inhibition of AICD in lymphocytes by the wild type, p.T56I and p.H122Y DcR3-Fc; Peripheral blood lymphocytes were activated with 1 µg/ml phytohaemagglutinin (PHA) for 24 hours and then were cultured in the presence of 100 U/ml interleukin-2 (IL-2) for 5 days. The activated lymphocytes were re-stimulated in plate-bond anti-human CD3 (1 µg/ml anti-human CD3 in PBS during plate coating) in the presence or absence of the wild type and both mutants (20 µg/ml) or PBS and Fc (10 µg/ml) as the controls of the experiment. (B) Inhibition of AICD in lymphocytes by various concentrations (indicated on the graph) of the wild type and both mutants; Graphs represent mean ± standard deviation (SD) of data obtaining from 5 different healthy donors. Statistical analyses were evaluated by Student *t*-test and the *p*-value less than 0.05 was considered as statistically significant (*$p<0.05$; **$p<0.01$; ***$p<0.001$).

Lymphocytes proliferation

It has been reported that DcR3 can enhance lymphocyte proliferation in conjunction with sub-optimal concentration of mitogens [19, 70, 71]. In this study, we determined whether the mutant DcR3 can enhance lymphocyte proliferation with sub-optimal concentration of immobilized anti-CD3 (50 ng/ml) comparing to the wild type. Both mutants can enhance lymphocyte proliferation with sub-optimal anti-CD3 activation. Interestingly, at the concentration of 40 μg/ml, both mutants significantly enhanced lymphocyte proliferation comparing to the wild type with the *p*-value of 0.045 and 0.035, respectively (figure 18B).

A

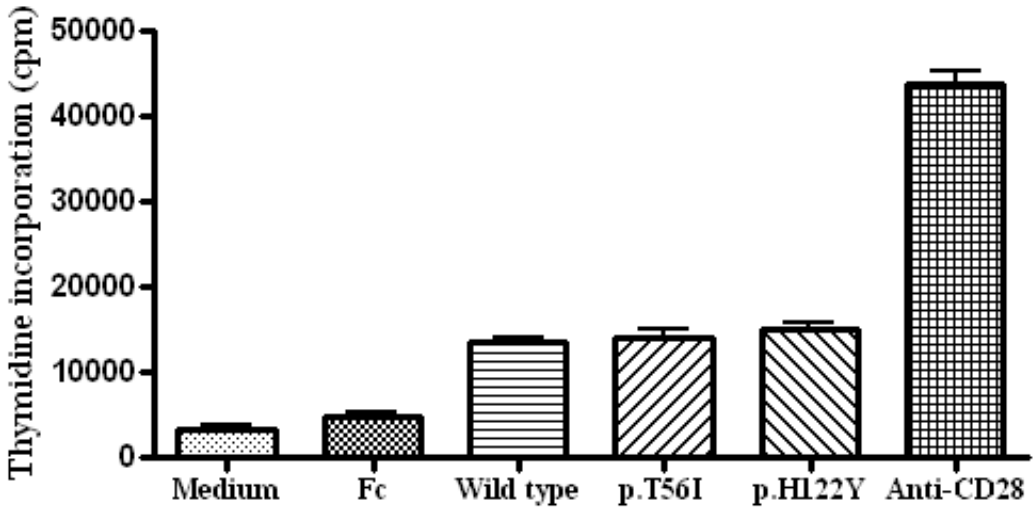

B

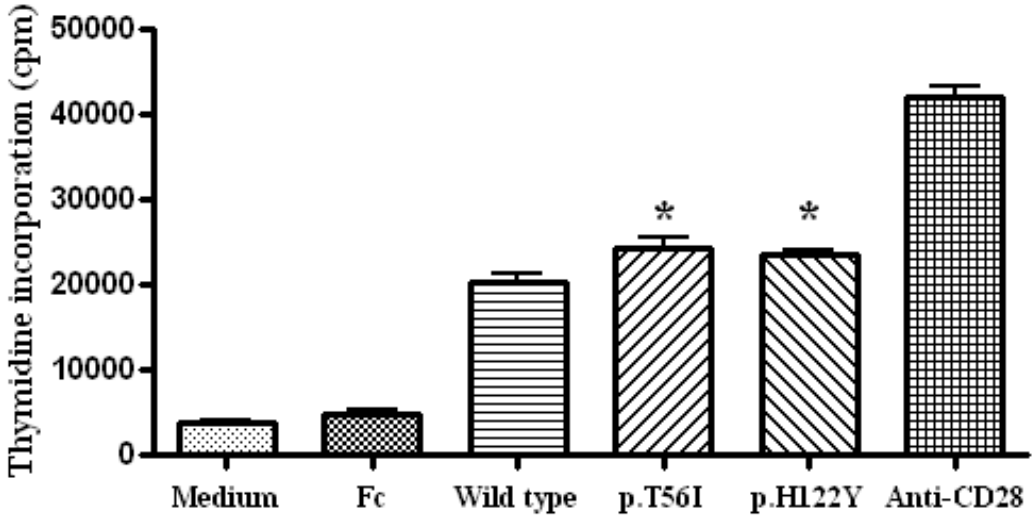

Figure 18. Lymphocyte proliferation; Lymphocytes were isolated from peripheral blood from 4 healthy controls. The cells ($2x10^5$ cells/well) were plated to sub-optimal anti-CD3 pre-coated plated (100 ul of 50 ng/ml anti-CD3 in PBS during plate coating) in the presence or absence of (A) 20 µg/ml or (B) 40 µg/ml of the wild type and both mutants or 10 µg/ml Fc and 1 µg/ml anti-CD28 as controls for the experiment and cultured for 72 hours. Then [^{3}H]thymidine (1.0 µCi/well) were added to the culture and incubated for 16 hours before cell harvesting. The [^{3}H]thymidine incorporation was measured by scintillation counter. Graphs represent mean ± standard deviation (SD) of data obtaining from 4 different healthy donors. Statistical analyses were evaluated by Student *t*-test and the *p*-value less than 0.05 was considered as statistically significant (*$p<0.05$; **$p<0.01$; ***$p<0.001$).

CHAPTER V

CONCLUSIONS AND DISCUSSIONS

Conclusions

For juvenile SLE patients, we, for the first time, found that those in active state had significantly increased levels of serum DcR3 comparing to those in inactive state and unaffected controls. Combined with previous evidences of the etiologic roles of DcR3 in SLE in mice, our finding suggests its roles in disease activity in human juvenile SLE.

In addition, we identified two heterozygous missense mutations of the *DcR3* gene in two unrelated SLE patients from a total of 200 unrelated SLE patients. The mutations were p.T56I and p.H122Y. Although both patients inherited the mutations from their unaffected mothers, many lines of evidence suggested that they might play a role in the pathologic mechanism of SLE. Both mutations changed polarity of the amino acid residues. The p.T56I was absent in 500 unaffected age and ethnic-matched controls (1,000 alleles), while the p.H122Y was found in heterozygous state in one control. The amino acid residue at position 56 of DcR3 showed evolutionarily conserved in all 14 vertebrate species available in NCBI database, while the residue at position 122 conserved among 5 mammalian species. Both mutations reside in the FasL binding domain in DcR3.

Due to these suggestive evidences, we decided to perform functional analyses to determine whether these DNA changes had any functions different from the wild-type. The affinity test by surface plasmon resonance (SPR) technique revealed that the p.T56I mutant had a 2.4 fold greater, whereas the p.H122Y mutant had 0.7 fold lower affinity to FasL comparing to the wild-type DcR3. However, the apoptosis assay by AnnexinV/PI staining showed that both p.T56I and p.H122Y mutants had no differences

of the ability to suppress FasL-induced Jurkat cell apoptosis and activation induced cell death in lymphocytes. Intriguingly, comparing to the wild-type DcR3, both p.T56I and p.H122Y mutants significantly enhanced lymphocyte proliferation under sub-optimal concentration of anti-CD3 stimulation.

In conclusion, we, for the first time, found that juvenile SLE patients in active state had significantly increased levels of serum DcR3 comparing to those in inactive state and unaffected controls. In addition, we identified two mutations in the *DcR3* gene that increased lymphocyte proliferation compared to the wild-type. These suggest that DcR3 might play an etiologic role in human SLE pathogenesis, either by an increased amount or an altered structure.

Discussions

Previous reports suggested an involvement of DcR3 in adult SLE development. This led us to investigate whether DcR3 also played an etiologic role in juvenile SLE. We first used the ELISA technique to determine the level of serum DcR3 in 61 juvenile SLE patients. There was a trend of an increase in serum DcR3 level in patients (181.7 pg/ml) comparing to controls (65.52 pg/ml), although the difference was not statistically significantly different (p = 0.219). This could be because of the inadequate number of patients leading to an inadequate power to reveal statistical significance.

Subsequently, we studied the serum DcR3 level in subgroups of patients. Patients with SLEDAI scores of less than 10 were classified as inactive while at least 10 as active. The active group showed a significant increase of serum DcR3 level in comparison to the inactive (p = 0.003) and unaffected controls (p = 0.001). This is consistent to the previous studies in adult SLE [17,19], and suggests that increased serum DcR3 level is associated with activity of juvenile SLE.

Although the increased level serum DcR3 was found to be associated with active SLE, approximately half (30 out of 61; 49%) of our juvenile SLE patients and similar percentage from previous studies [17,19] had undetectable serum DcR3 levels. In theory, a structural change leading to an increased activity of DcR3 might have similar effects to an increased amount of a normal structure DcR3. We therefore hypothesized that a proportion of these patients might have a DcR3 gain-of-function mutation.

PCR-sequencing the entire coding regions of DcR3 in 200 unrelated SLE patients revealed two missense mutations in heterozygous state, each in a patient. They were p.T56I and p.H122Y. Although both patients inherited the mutations from their unaffected mothers, many lines of evidence suggested that they might play a role in the development of SLE. First, both mutations changed polarity of the amino acid residues; the p.T56I changes the amino acid residue 56 from threonine, an uncharged polar amino acid to isoleucine, a nonpolar amino acid. The p.H122Y changes the amino acid residue 122 from histidine, a positively charged amino acid to tyrosine, an uncharged polar amino acid. Second, the p.T56I was absent in 500 unaffected age and ethnic-matched controls (1,000 alleles), while the p.H122Y was found in heterozygous state in one control. Third, the amino acid residue in position 56 of DcR3 was evolutionarily conserved in all 14 vertebrate species available in Ensembl database, while the 122 was conserved among 5 mammalian species. Fourth, both mutations reside in the FasL binding domain in DcR3. DcR3 contains 300 amino acid residues, while the FasL binding domain is 43 amino acid residues. The probability of any two DNA changes reside in this domain is 0.14x0.14= 2%.

Due to these suggestive evidences, we decided to perform functional analyses to determine whether these DNA changes had any functions different from the wild-type. Because both resided in the FasL binding domain, we first performed the affinity test by surface plasmon resonance (SPR) technique. Our study revealed the affinity of the wild-type DcR3-Fc to FasL with the Kd of 128±1.1 nM which was 2.1 fold

greater than the affinity from a previous study [67] with the Kd of 271.4±24.4 nM. This suggests that the difference in domain components of DcR3 might have an effect on its affinity to FasL. In this study, we constructed full length DcR3 with Fc tag; whereas the previous study [67] constructed only cysteine-rich domains DcR3 (V30-S195) with poly-histidine tag lacking of the signal peptide domain and heparan binding domain. Therefore, the unequal domain contents in DcR3 between our study and previous study [67] might lead to the difference in affinity. Regardless, the binding constant value (Kd) of our study was in the similar scale of concentration (nM) to the previous study [67]. Although there has been only the modeling of DcR3:TL1A interaction indicating DcR3 used cysteine-rich domain (CRD) to bind to TL1A molecule, the L85A/R89D double mutant in cysteine-rich domain 2 (CRD2) of DcR3 showed dramatically decreased affinities to TL1A as well as LIGHT and FasL [67]. Of note, this suggests that TL1A, LIGHT and FasL might share the same binding domain to DcR3 molecule.

Using the SPR technique on our two mutants, we found that the p.T56I mutant had a 2.4 fold greater, whereas the p.H122Y mutant had 0.7 fold lower affinity to FasL comparing to the wild-type DcR3. Interestingly, the affinity changes of these two mutations move to the opposite direction. Nonetheless, the possibility of both ways playing a role in SLE pathogenesis remains. Lymphocytes might have an increased apoptosis leading to increased autoantigen production in SLE [72, 73]. On the contrary, a lower apoptosis could also lead to promote survival of activated lymphocytes in SLE [16, 19].

When FasL binds to its receptors on lymphocytes, it will lead to apoptosis [74]. DcR3 is a decoy, binding to FasL. With less available FasL, lymphocytes are expected to have less apoptosis. We did the apoptosis assay by AnnexinV/PI staining. It showed that both p.T56I and p.H122Y mutants had no differences of the ability to suppress FasL-induced Jurkat cell apoptosis and activation induced cell death in lymphocytes. This suggests that DcR3 might not play a role in SLE pathogenesis through FasL pathway.

As previously discussed, pathogenesis of SLE could involve either apoptosis or proliferation of lymphocytes. In addition, many molecules besides FasL might be able to bind to the same domain of DcR3. We therefore moved from apoptosis to proliferation assays. Intriguingly, comparing to the wild-type DcR3, both p.T56I and p.H122Y mutants significantly enhanced lymphocyte proliferation under sub-optimal concentration of anti-CD3 stimulation. For the first time, we have identified germ-line mutations in *DcR3* with a functional change in SLE patients.

To confirm their etiologic roles in SLE, many experiments could be further performed. The study of proliferation of lymphocytes directly drawn from these two SLE patients with the DcR3 mutations as well as their unaffected mothers would tell whether the mutations have the effect on its protein function *in vivo* and SLE pathogenesis. If it shows the effect only on the SLE patients but not their mothers, it would strengthen their pathogenic role in these cases. The fact that *DcR3*-transgenic mice developed SLE-like syndrome with higher penetrance in female than in male [16, 17] and SLE is a multi-factorial disease which the genetic factor more contributes to the disease when it occurs in male, mutant *DcR3*-transgenic mice would be a way to demonstrate the SLE phenotype in mice and investigate whether mutant *DcR3*-transgenic mice develop SLE in balance sex ratio. In addition, there was one study indicated DcR3 was regulated by female sex hormones in endometrial cells *in vitro* and the cyclic change pattern of serum DcR3 during menstruation [75]. This knowledge might link to the fact that SLE has higher prevalence in female than male according to DcR3 regulated by female sex hormones.

The mechanism that DcR3 co-stimulates lymphocyte activation has not been clearly elucidated. Although there were studies showing that DcR3 enhanced mouse and human T cell proliferation [71] but not soluble Fas [19, 70] as well as soluble LIGHT had a potential to block co-stimulation ability of DcR3 in T cells [70]. This suggests that LIGHT is likely a ligand involving in DcR3 co-stimulation in T cell proliferation. Although LIGHT is a molecule expressed on activated T cells and

transduces its signal through HVEM receptor on T cells by T-T cell interaction leading to enhanced T-cell activation [62], in addition to LIGHT-HVEM transduction, one study postulated that DcR3 bound to LIGHT on activated mouse T cells and co-stimulated T cell proliferation indicating LIGHT in turn could act as a receptor transmitting the DcR3 signal into T cell [71]. It seems to be perplexed that either DcR3 or LIGHT itself can enhance T cell proliferation; while the soluble LIGHT can block the ability of DcR3 to increase T cell proliferation as well as LIGHT itself would be a receptor for signal transduction on T cells via DcR3 ligation. In addition to LIGHT, we cannot exclude the possibility that DcR3 might transduce the signal through the other so far unidentified molecules than LIGHT. These possible underlying mechanisms need to be further elucidated.

Of relevant to our studies, we identified the mutations in the *DcR3* gene that affected its protein function. Both mutant DcR3 enhanced co-stimulation of lymphocyte proliferation (figure 18). If LIGHT is a key molecule relevant to the process of DcR3 co-stimulation in lymphocytes, the mutations might also affect the interaction of DcR3 and LIGHT. Therefore, the affinity test of mutant DcR3 to LIGHT would be further performed to elucidate this issue. In addition, lymphocytes consist of B and T cells which produce cytokine and antibody and the aberrant apoptosis and proliferation of both cell types play an role in autoimmunity [11, 45, 53, 62, 73]. It would be interesting to study apoptosis and proliferation test in B and T cell subpopulations and determine whether both mutants change an ability in apoptosis and proliferation compared to the wild type. SLE is a multi-factorial disorder in which several genes could play a significant role in disease pathogenesis. In the fact that mutant DcR3 exhibited small magnitude of effect on enhanced lymphocyte proliferation (figure 18) and the mutations were present in unaffected mothers of the SLE patients, it remains possible that there might be some other gene defects in combination with the *DcR3* gene mutations playing an etiologic role in SLE.

In conclusion, we, for the first time, found that juvenile SLE patients in active state had significantly increased levels of serum DcR3 comparing to those in inactive state and unaffected controls. In addition, we identified two mutations in the *DcR3* gene that increased lymphocyte proliferation compared to the wild-type. These suggest that DcR3 might play an etiologic role in human SLE pathogenesis, either by an increased amount or an altered structure.

REFERENCES

[1] D'Cruz, D.P., M.A. Khamashta, and G.R. Hughes, *Systemic lupus erythematosus.* Lancet, 369,9561(2007):587-96.

[2] Pluchinotta, F.R., et al., *Distinctive clinical features of pediatric systemic lupus erythematosus in three different age classes.* Lupus, 16,8(2007):550-5.

[3] Danchenko, N., J.A. Satia, and M.S. Anthony, *Epidemiology of systemic lupus erythematosus: a comparison of worldwide disease burden.* Lupus, 15,5(2006):308-18.

[4] Malleson, P.N., M.Y. Fung, and A.M. Rosenberg, *The incidence of pediatric rheumatic diseases: results from the Canadian Pediatric Rheumatology Association Disease Registry.* J Rheumatol, 23,11(1996):1981-7.

[5] McCarty, D.J., et al., *Incidence of systemic lupus erythematosus. Race and gender differences.* Arthritis Rheum, 38,9(1995):1260-70.

[6] Tsokos, G.C., *Systemic lupus erythematosus.* N Engl J Med, 365,22(2011):2110-21.

[7] Simard, J.F., et al., *Exposure to maternal smoking and incident SLE in a prospective cohort study.* Lupus, 18,5(2009):431-5.

[8] Tsokos, G.C., I.T. Magrath, and J.E. Balow, *Epstein-Barr virus induces normal B cell responses but defective suppressor T cell responses in patients with systemic lupus erythematosus.* J Immunol, 131,4(1983):1797-801.

[9] Kang, I., et al., *Defective control of latent Epstein-Barr virus infection in systemic lupus erythematosus.* J Immunol, 172,2(2004):1287-94.

[10] Poole, B.D., et al., *Epstein-Barr virus and molecular mimicry in systemic lupus erythematosus.* Autoimmunity, 39,1(2006):63-70.

[11] Cohen-Solal, J.F., et al., *Hormonal regulation of B-cell function and systemic lupus erythematosus.* Lupus, 17,6(2008):528-32.

[12] Sequeira, J.F., et al., *Systemic lupus erythematosus: sex hormones in male patients.* Lupus, 2,5(1993):315-7.

[13] Criswell, L.A., *The genetic contribution to systemic lupus erythematosus.* Bull NYU Hosp Jt Dis, 66,3(2008):176-83.

[14] Rhodes, B. and T.J. Vyse, *General aspects of the genetics of SLE.* Autoimmunity, 40,8(2007):550-9.

[15] Janeway, C.A.T., Paul; Walport, Mark; Shlomchik, Mark, *Immunobiology*. 5th ed. (2001):Garland Science.

[16] Han, B., et al., *Overexpression of human decoy receptor 3 in mice results in a systemic lupus erythematosus-like syndrome.* Arthritis Rheum, 56,11(2007):3748-58.

[17] Han, B., et al., *DcR3 as a diagnostic parameter and risk factor for systemic lupus erythematosus.* Int Immunol, 20,8(2008):1067-75.

[18] Otsuki, T., et al., *Over-expression of the decoy receptor 3 (DcR3) gene in peripheral blood mononuclear cells (PBMC) derived from silicosis patients.* Clin Exp Immunol, 119,2(2000):323-7.

[19] Lee, C.S., et al., *Elevated serum decoy receptor 3 with enhanced T cell activation in systemic lupus erythematosus.* Clin Exp Immunol, 151,3(2008):383-90.

[20] Hahne, M., et al., *Characterization of the non-functional Fas ligand of gld mice.* Int Immunol, 7,9(1995):1381-6.

[21] Russell, J.H., et al., *Mature T cells of autoimmune lpr/lpr mice have a defect in antigen-stimulated suicide.* Proc Natl Acad Sci U S A, 90,10(1993): 4409-13.

[22] Mysler, E., et al., *The apoptosis-1/Fas protein in human systemic lupus erythematosus.* J Clin Invest, 93,3(1994):1029-34.

[23] McNally, J., et al., *Fas ligand expression and function in systemic lupus erythematosus.* J Immunol, 159,9(1997):4628-36.

[24] Tamada, K., et al., *Cutting edge: selective impairment of CD8+ T cell function in mice lacking the TNF superfamily member LIGHT.* J Immunol, 168,10(2002):4832-5.

[25] Wang, E.C., et al., *DR3 regulates negative selection during thymocyte development.* Mol Cell Biol, 21,10(2001):3451-61.

[26] Petri, M., *Epidemiology of systemic lupus erythematosus.* Best Pract Res Clin Rheumatol, 16,5(2002):847-58.

[27] Han, S., et al., *Evaluation of imputation-based association in and around the integrin-alpha-M (ITGAM) gene and replication of robust association between a non-synonymous functional variant within ITGAM and systemic lupus erythematosus (SLE).* Hum Mol Genet, 18,6(2009): 1171-80.

[28] Cappola, T.P., et al., *Loss-of-function DNA sequence variant in the CLCNKA chloride channel implicates the cardio-renal axis in interindividual heart failure risk variation.* Proc Natl Acad Sci U S A, 108,6(2011):2456-61.

[29] Lee-Kirsch, M.A., et al., *Mutations in the gene encoding the 3'-5' DNA exonuclease TREX1 are associated with systemic lupus erythematosus.* Nat Genet, 39,9(2007):1065-7.

[30] Harley, J.B., et al., *The genetics of human systemic lupus erythematosus.* Curr Opin Immunol, 10,6(1998):690-6.

[31] Kelley, J., et al., *Variation in the relative copy number of the TLR7 gene in patients with systemic lupus erythematosus and healthy control subjects.* Arthritis Rheum, 56,10(2007):3375-8.

[32] Blanchong, C.A., et al., *Genetic, structural and functional diversities of human complement components C4A and C4B and their mouse homologues, Slp and C4.* Int Immunopharmacol, 1,3(2001):365-92.

[33] Niederer, H.A., et al., *FcgammaRIIB, FcgammaRIIIB, and systemic lupus erythematosus.* Ann N Y Acad Sci, 1183(2010):69-88.

[34] Lu, R., et al., *Genetic associations of LYN with systemic lupus erythematosus.* Genes Immun, 10,5(2009):397-403.

[35] Lee, H.S., et al., *Genetic risk factors for rheumatoid arthritis differ in Caucasian and Korean populations.* Arthritis Rheum, 60,2(2009):364-71.

[36] Kochi, Y., et al., *Genetics of rheumatoid arthritis: underlying evidence of ethnic differences.* J Autoimmun, 32,3-4(2009):158-62.

[37] Nath, S.K., et al., *A nonsynonymous functional variant in integrin-alpha(M) (encoded by ITGAM) is associated with systemic lupus erythematosus.* Nat Genet, 40,2(2008):152-4.

[38] Harley, J.B., et al., *Genome-wide association scan in women with systemic lupus erythematosus identifies susceptibility variants in ITGAM, PXK, KIAA1542 and other loci.* Nat Genet, 40,2(2008):204-10.

[39] Hom, G., et al., *Association of systemic lupus erythematosus with C8orf13-BLK and ITGAM-ITGAX.* N Engl J Med, 358,9(2008):900-9.

[40] Sanchez-Guerrero, J., et al., *Postmenopausal estrogen therapy and the risk for developing systemic lupus erythematosus.* Ann Intern Med, 122,6(1995):430-3.

[41] Meier, C.R., et al., *Postmenopausal estrogen replacement therapy and the risk of developing systemic lupus erythematosus or discoid lupus.* J Rheumatol, 25,8(1998):1515-9.

[42] Garcia, B.A., et al., *Resetting the epigenetic histone code in the MRL-lpr/lpr mouse model of lupus by histone deacetylase inhibition.* J Proteome Res, 4,6(2005):2032-42.

[43] Mishra, N., et al., *Histone deacetylase inhibitors modulate renal disease in the MRL-lpr/lpr mouse.* J Clin Invest, 111,4(2003):539-52.

[44] Ballestar, E., M. Esteller, and B.C. Richardson, *The epigenetic face of systemic lupus erythematosus.* J Immunol, 176,12(2006):7143-7.

[45] Salmon, M. and C. Gordon, *The role of apoptosis in systemic lupus erythematosus.* Rheumatology (Oxford), 38,12(1999):1177-83.

[46] Wu, J., et al., *Fas ligand mutation in a patient with systemic lupus erythematosus and lymphoproliferative disease.* J Clin Invest, 98,5(1996):1107-13.

[47] Fisher, G.H., et al., *Dominant interfering Fas gene mutations impair apoptosis in a human autoimmune lymphoproliferative syndrome.* Cell, 81,6(1995):935-46.

[48] Rieux-Laucat, F., et al., *Mutations in Fas associated with human lymphoproliferative syndrome and autoimmunity.* Science, 268,5215(1995):1347-9.

[49] Wu, J., et al., *FAS mRNA editing in Human Systemic Lupus Erythematosus.* Hum Mutat, 32,11(2011):1268-77.

[50] Cohen, P.L. and R.A. Eisenberg, *Lpr and gld: single gene models of systemic autoimmunity and lymphoproliferative disease.* Annu Rev Immunol, 9(1991):243-69.

[51] Watanabe-Fukunaga, R., et al., *Lymphoproliferation disorder in mice explained by defects in Fas antigen that mediates apoptosis.* Nature, 356,6367(1992):314-7.

[52] Takahashi, T., et al., *Generalized lymphoproliferative disease in mice, caused by a point mutation in the Fas ligand.* Cell, 76,6(1994):969-76.

[53] Zhang, J., X. Xu, and Y. Liu, *Activation-induced cell death in T cells and autoimmunity.* Cell Mol Immunol, 1,3(2004):186-92.

[54] Kabelitz, D. and O. Janssen, *Antigen-induced death of T-lymphocytes.* Front Biosci, 2(1997):d61-77.

[55] Pitti, R.M., et al., *Genomic amplification of a decoy receptor for Fas ligand in lung and colon cancer.* Nature, 396,6712(1998):699-703.

[56] Yu, K.Y., et al., *A newly identified member of tumor necrosis factor receptor superfamily (TR6) suppresses LIGHT-mediated apoptosis.* J Biol Chem, 274,20(1999):13733-6.

[57] Migone, T.S., et al., *TL1A is a TNF-like ligand for DR3 and TR6/DcR3 and functions as a T cell costimulator.* Immunity, 16,3(2002):479-92.

[58] Siegel, R.M., et al., *The multifaceted role of Fas signaling in immune cell homeostasis and autoimmunity.* Nat Immunol, 1,6(2000):469-74.

[59] Funke, B., et al., *Functional characterisation of decoy receptor 3 in Crohn's disease.* Gut, 58,4(2009):483-91.

[60] Hayashi, S., et al., *Decoy receptor 3 expressed in rheumatoid synovial fibroblasts protects the cells against Fas-induced apoptosis.* Arthritis Rheum, 56,4(2007):1067-75.

[61] Green, D.R., *Apoptosis. Death deceiver.* Nature, 396,6712(1998):629-30.

[62] Wang, J., et al., *The regulation of T cell homeostasis and autoimmunity by T cell-derived LIGHT.* J Clin Invest, 108,12(2001):1771-80.

[63] Zhan, C., et al., *Biochemical and structural characterization of the human TL1A ectodomain.* Biochemistry, 48,32(2009):7636-45.

[64] Bamias, G., et al., *Role of TL1A and its receptor DR3 in two models of chronic murine ileitis.* Proc Natl Acad Sci U S A, 103,22(2006):8441-6.

[65] Young, H.A. and M.G. Tovey, *TL1A: a mediator of gut inflammation.* Proc Natl Acad Sci U S A, 103,22(2006):8303-4.

[66] Yang, C.R., et al., *Soluble decoy receptor 3 induces angiogenesis by neutralization of TL1A, a cytokine belonging to tumor necrosis factor superfamily and exhibiting angiostatic action.* Cancer Res, 64,3(2004):1122-9.

[67] Zhan, C., et al., *Decoy strategies: the structure of TL1A:DcR3 complex.* Structure, 19,2(2011):162-71.

[68] Akkahat, P., et al., *Surface-grafted Poly(acrylic acid) Brushes as a Precursor Layer for Biosensing Applications: Effect of Graft Density and Swellability on the Detection Efficiency.* Langmuir, (2011).

[69] Hayashi, S., et al., *Decoy receptor 3 is highly expressed in patients with rheumatoid arthritis.* Mod Rheumatol, 20,1(2009):63-8.

[70] Wan, X., et al., *A TNF family member LIGHT transduces costimulatory signals into human T cells.* J Immunol, 169,12(2002):6813-21.

[71] Shi, G., et al., *Mouse T cells receive costimulatory signals from LIGHT, a TNF family member.* Blood, 100,9(2002):3279-86.

[72] Dhir, V., et al., *Increased T-lymphocyte apoptosis in lupus correlates with disease activity and may be responsible for reduced T-cell frequency: a cross-sectional and longitudinal study.* Lupus, 18,9(2009):785-91.

[73] Lorenz, H.M., et al., *In vitro apoptosis and expression of apoptosis-related molecules in lymphocytes from patients with systemic lupus erythematosus and other autoimmune diseases.* Arthritis Rheum, 40,2(1997):306-17.

[74] Strand, S., et al., *Lymphocyte apoptosis induced by CD95 (APO-1/Fas) ligand-expressing tumor cells--a mechanism of immune evasion?* Nat Med, 2,12(1996):1361-6.

[75] Chen, H.F., et al., *Decoy receptor 3 expression during the menstrual cycle and pregnancy, and regulation by sex steroids in endometrial cells in vitro.* Hum Reprod, 24,6(2009):1350-8.

APPENDIX

APPENDIX

BUFFERS AND REAGENTS

1. 20 mM Sodium Phosphate buffer pH7.0

0.5 M NaH_2PO_4	18.64	ml
0.5 M Na_2HPO_4	21.36	ml
dH_2O to volume	1,000	ml

The buffer will be pH 7.0 at $25^{O}C$

2. 0.1 M Glycine-HCl buffer pH 2.7

Glycine	11.1	g
dH2O	800	ml

Adjust pH with conc. HCl until the pH is 2.7 then add water to volume 1,000 ml

3. 1.0 M Tris-HCl buffer pH9.0

Tris base	121.1	g
dH_2O	800	ml

Adjust pH with conc. HCl until the pH is 9.0 then add water to volume 1,000 ml

4. Phosphate buffer saline (PBS) pH7.4

NaCl	8.0	g
Na_2HPO_4	0.2	g
KCl	1.44	g
KH_2PO_4	0.24	g
dH_2O	800	ml

Adjust pH with conc. HCl until the pH is 7.4 then add water to volume 1,000 ml

5. 10X Tris buffer saline (TBS) pH7.4

Tris base	61	g
NaCl	90	g
dH_2O	800	ml

Adjust pH with conc. HCl until the pH is 7.4 then add water to volume 1,000 ml

6. 10X Tris Glycine buffer pH8.3

Tris base	6.05	g
Glycine	147.1	g
dH_2O to volume	1,000	ml

Heat to dissolve the buffer then the pH will be 8.3 at $25^{O}C$

7. 10% SDS

Sodium dodecyl sulfate	10	g
dH_2O to volume	1,000	ml

8. SDS-PAGE running buffer

10X Tris-Glycine buffer pH8.3	100	ml
10% SDS	10	ml
dH_2O to volume	1,000	ml

9. Transfer buffer

10X Tris-Glycine buffer pH8.3	100	ml
Methanol	200	ml
dH_2O to volume	1,000	ml

10. 0.5% TBS-T

10X TBS	100	ml
Tween-20	500	ul
dH_2O to volume	1,000	ml

11. 5% Blocking buffer

Non fat dry milk	5	g
0.5% TBS-T to volume	100	ml

Agitate to dissolve the buffer

12. 0.5 M EDTA pH8.0

Ethylenediaminetetraacetic acid	146.1	g
dH2O	800	ml

Adjust pH with NaOH pellet until the pH is 8.0 then add water to volume 1,000 ml

13. 10X TBE buffer pH8.0

Tris-base	108	g
Boric acid	55	g
0.5 M EDTA pH8.0	40	ml
dH_2O to volume	1,000	ml

14. LB agar

Tryptone	10	g
Yeast extract	5	g

NaCl	10	g
Agar	15	g
dH_2O to volume	1,000	ml

Autoclave to sterilize the media

15. LB broth

Tryptone	10	g
Yeast extract	5	g
NaCl	10	g
dH_2O to volume	1,000	ml

Autoclave to sterilize the media

BIOGRAPHY

Mr. Chayanin Chokdeemeeboon was born in April 24th, 1983. He grew up in the Buddhism family and he is a middle son of Mr. Chansak and Mrs. Prapawan Chokdeemeeboon with two sisters. He studied in primary and secondary school at Sarasaspittaya School then he studied in high school at Watsuthiwararam School. He got a scholarship from Development and Promotion of Science and Technology Talents Project while he was studying in Faculty of Science, Chulalongkorn University during 2002 - 2005. He graduated in Bachelor of Sciences in Botany with 2nd class honor. Then Professor Apiwat Mutirangura gave him an opportunity to study in Ph.D. program of Biomedical Sciences at Chulalongkorn University since 2007 under supervision of Professor Vorasuk Shotelersuk and Associate Professor Kanya Suphapeetiporn. During his Ph.D. study, he got 72th Anniversary of His Majesty the King Bhumibol Adulyadej at first year then he had got Dutsadi Phiphat Scholarship since 2008. In 2011, he got an opportunity of going to University of Liverpool, United Kingdom in the period of 7 months to perform some parts of this dissertation and molecular techniques training under supervision of Professor Steven Edwards.

Publications

1. *DcR3* mutations leading to enhanced lymphocyte proliferation in SLE patients. Chokdeemeeboon C, Ammarinthnukrowh P, Tongkobpetch S, Srichomtong C, Deekajorndech T, Rianthavorn P, Kingwattanakul P, Avihingsanon Y, Wright H, Akkahat P, Hoven VP, Edwards S, Hirankarn N, Suphapeetiporn K, Shotelersuk V. (Manuscript in preparation)
2. Interleukin-10 expression and promoter polymorphisms in pediatric patients with systemic lupus erythematosus. Rianthavorn P, Chokedeemeeboon C, Deekajorndech T, Shotelersuk V, Suphapeetiporn K. (Manuscript in preparation)
3. *FGFR1* and *FGFR2* mutations in Thai Patients with Pfeiffer Syndrome. Chokdeemboon C, Mahatumarat C, Rojvachiranonda N, Tongkobpetch S, Suphapeetiporn K, Shotelersuk V. (Manuscript submitted)